IEEE Journal of Microwaves

Received 5 October 2022; revised 27 November 2022; accepted 2 December 2022. Date of publication 27 December 2022; date of current version 6 January 2023.

Digital Object Identifier 10.1109/JMW.2022.3228118

THz Systems Exploiting Photonics and Communications Technologies

JAN C. BALZER [1] (Member, IEEE), CLARA J. SARACENO [2], MARTIN KOCH [3], PRIYANSHA KAURAV [4], ULLRICH R. PFEIFFER [4] (Fellow, IEEE), WITHAWAT WITHAYACHUMNANKUL [5] (Senior Member, IEEE), THOMAS KÜRNER [6] (Fellow, IEEE), ANDREAS STÖHR [7] (Senior Member, IEEE), MOHAMMED EL-ABSI [8], ALI AL-HAJ ABBAS [8], THOMAS KAISER [8] (Senior Member, IEEE), AND ANDREAS CZYLWIK [1]

(Invited Paper)

[1]Chair of Communication Systems, University of Duisburg-Essen, 47057 Duisburg, Germany
[2]Photonics and Ultrafast Laser Science, Ruhr Universität Bochum, 44801 Bochum, Germany
[3]Department of Physics and Material Sciences Center, Philipps-Universität Marburg, 35032 Marburg, Germany
[4]Institute for High-Frequency and Communication Technology, University of Wuppertal, 42119 Wuppertal, Germany
[5]Terahertz Engineering Laboratory, The University of Adelaide, Adelaide, SA 5005, Australia
[6]Institut für Nachrichtentechnik, Technische Universität Braunschweig, 38106 Braunschweig, Germany
[7]Department of Optoelectronics, University of Duisburg-Essen, 47057 Duisburg, Germany
[8]Institute of Digital Signal Processing, University of Duisburg–Essen, 47057 Duisburg, Germany

CORRESPONDING AUTHOR: Jan C. Balzer (e-mail: jan.balzer@uni-due.de).

This work did not involve human subjects or animals in its research.

ABSTRACT Terahertz (THz) systems open up the possibility of new applications of electromagnetic waves. Enormous bandwidths up to several terahertz enable the development of powerful spectroscopy systems that can provide insights into the structure and material of objects with micrometer resolution. New high power and compact THz time-domain spectroscopy (TDS) systems will be presented. The wide bandwidth also enables high-resolution imaging under far-field conditions to analyze arbitrary objects from a distance. In addition, a near-field system-on-a-chip imaging system is presented that achieves a resolution of 10 μm. Additionally, the application of terahertz waves presents challenges due to the low transmit power of the sources, high attenuation in free space, and the high noise figures of the receivers. These challenges can be overcome by antennas with high gain. Since - depending on the application - spatial scanning or focusing in a time-varying direction is required, beam steering is an essential component of many THz systems. In terms of communications, terahertz carrier frequencies offer wide bandwidths, enabling correspondingly high data rates of 100 Gbit/s and more. As a result, the frequency bands between 250 GHz and 450 GHz have already been identified and/or allocated for communication services and are being discussed as a component of 6G mobile communications. Concepts and demonstrations for 6G terahertz mobile communications will be presented. The high bandwidth of terahertz waves can also be used for high-accuracy indoor localization.

INDEX TERMS THz time-domain spectroscopy, high average power THz systems, THz far-field imaging, THz near-field imaging, THz communication, THz localization, MTT 70th Anniversary Special Issue.

I. INTRODUCTION

Terahertz (THz) systems are currently undergoing a transformation from pure basic research to application-driven research [1], [2]. In the following, systems dealing with the frequency range from 0.1 THz to 10 THz are referred to as THz systems. Before discussing the present and future of THz systems, a brief history will be given here. An important pioneer of high frequency technology is Bose, who already in 1899 described the nonlinearity of junctions similar to modern diodes [3]. Besides this early success of electronics, the development of a far infrared (FIR) spectrometer by Rubens and Nichols 1897 provided a breakthrough [4]: Planck was able to use the measured data to develop Planck's radiation law. Already in 1925, the gap between the FIR and

electric sources could be closed by overlapping the radiation of a Hertzian oscillator with a mercury arc source [5]. Other important inventions that are still used today are the Golay cell from 1947 [6] and the cooled bolometer from 1942 [7]. As early as 1954, microwave spectroscopy could be extended into the submillimeter range, thus realizing also spectroscopically the transition to the FIR range [8]. A major advance for spectroscopy in the FIR range is Fourier transform spectroscopy (FTS) [9] which was ultimately only made possible by the development of computers and especially the fast Fourier transform (FFT) in 1965 [10]. In 1953, the development of the first backward wave oscillator (BWO) laid the foundation for electronic source above 300 GHz [11]. Coherent optical sources based on the laser principle were first demonstrated in 1964 in the form of the water vapor laser [12]. A major contribution to the development of modern laser-based spectroscopy systems represents the dispersive Fourier-transform spectroscopy (DFTS) [13], which laid the foundation for time-domain spectroscopy (TDS). TDS was used in the microwave regime as early as 1968 [14]. In 1970, the THz optical excited gas laser was developed, which is still widely used today [15]. The steady development of lasers and nonlinear elements such as electro-optical crystals [16] and the so-called Auston switch [17] led to the foundation of the very successful THz-TDS. Another application area responsible for significant advances in THz technology not covered in this article is astronomy [19]. An overview of THz space instruments is given by Siegel [18].

In the following, 5 relevant groups of THz systems will be considered in more detail. Section II deals with broadband spectroscopy systems based on the THz-TDS principle. Here, systems with high average power and compact systems are presented. Section III focuses on free-form imaging systems and integrated nearfield imaging systems. Section IV gives an overview of beam steering systems as enabling technology for imaging, communication, and localization. In Section V communication systems are presented. The focus is on standardization and regulation as well as mobile 6G THz communications. Section VI exhibits an indoor localization system based on low-complexity and energy-autonomous infrastructure.

II. BROADBAND SPECTROSCOPY SYSTEMS

A. TERAHERTZ TIME-DOMAIN SPECTROSCOPY

Terahertz time-domain spectroscopy was developed in the late 1980s as a tool for the THz frequency range [20]. This frequency range was difficult to access until then because the frequency is too low for optical light sources and too high for electronic microwave systems. THz-TDS is characterized by being an extremely broadband technique and being field resolved – i.e., providing a direct measurement of the THz electric field. This allows on the one hand for the complex permittivity of materials to be determined over a wide frequency range with a single measurement; on the other hand enables measurements with very high sensitivity compared to other

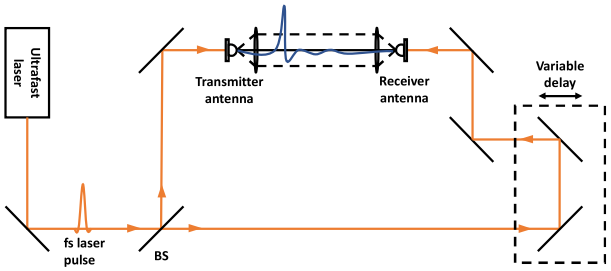

FIGURE 1. A simplified block diagram of a THz-TDS system. The optical pulse is split by a beam splitter (BS) into two arms: Transmitter and receiver arm. A variable delay is used in the receiver arm to allow optical sampling of the THz transient.

techniques such as Fourier-transform infrared spectroscopy (FTIR) [21].

The principle of operation of a THz-TDS is shown in Fig. 1 for the case of one of the most used THz-emitters for this technique: the photoconductive antenna (PCA) or Auston switch. In this scheme, an ultrafast laser emits a series of pulses that excite charge carriers in a semiconductor-based antenna with an ultrashort carrier lifetime [22]. The PCA acts as a transmitter when a bias voltage is applied to the antenna structure: The generated carriers are accelerated by the external bias field and emit electromagnetic radiation. The electromagnetic radiation is broadband and has spectral components from nearly 0 THz to several THz. The THz radiation can also be detected with a PCA driven by the same ultrafast laser: Here, the THz transient itself acts as an electric field accelerating the photoexcited charge carriers, and the photocurrent is proportional to the field amplitude. Since the optical pulse is shorter than the THz transient, it can be used for optical sampling. For this purpose, a variable delay is required in the receiver arm. Spectral data from the time domain signal can be obtained by Fourier transform [23]. It is important to note that the TDS technique relies on the generated THz pulses being phase-stable, since it requires multiple consequent pulses to reconstruct a single pulse.

PCAs are most used emitters and receivers in commercial systems, but several other techniques are nowadays also being increasingly deployed both in scientific applications and in more applied scenarios. The most prominently used method is optical rectification (OR) in $\chi^{(2)}$ nonlinear crystals. OR is a second order nonlinear effect, which was demonstrated as early as 1962 [24] closely after the invention of the laser. It is the quasi-DC component of the second order nonlinear polarization, which follows the envelope of the excitation femtosecond pulse, and acts as a source for the emission of THz radiation. The most crucial design constraints of THz sources based on optical rectification are: (1) reaching sufficiently high intensity with the driving laser on the nonlinear crystal to access the nonlinear response of the crystal while avoiding damage and other detrimental effects (2) achieving velocity matching conditions between the excitation and

the generated broadband THz wave over a reasonable length of the nonlinear crystal in order to efficiently convert the near infrared (NIR) light to a broadband THz pulse (3) generating sufficiently broad THz radiation and circumventing problems related to THz absorption to due inevitable phonon resonances.

Other emerging techniques to generate broadband THz pulses that could emerge in future THz systems include THz spintronic emitters [25], organic crystals [26], and plasma-based two-color filament sources [27]. However so far, these remain so far rather specialized lab sources, and have still to find their way to robust industrially compatible systems.

The first THz systems were operated with mode-locked dye lasers [28]. These lasers are very cumbersome to handle and some of the dyes used are highly carcinogenic. Consequently, a major step towards reliable THz systems was the use of newly developed and more reliable solid-state lasers in the early 1990s. Particularly worth mentioning here is the titanium:sapphire laser, which enabled the reliable generation of 60 fs pulses as early as 1991 [29]. Driven by such a laser, hyperspectral images in the THz range could be acquired for the first time [30]. Although titanium:sapphire lasers are much more stable compared to dye lasers, they are still complex laser systems that require a multistep optical pumping process. A potentially more compact and simpler ultrashort pulse laser system was also developed in the early 1990s: the mode-locked fiber laser [31]. These lasers are characterized by a compact design (about the size of a conventional shoebox) and the emitted radiation can naturally be transported very well through optical fibers. However, it took until the late 2000s until the first fiber-coupled THz system based on a fiber laser was presented [32]. Nowadays, most commonly used commercial THz-TDS systems are based on such compact ultrafast fiber-laser sources and PCA emitters and receivers, which demonstrate very high dynamic range operation [33].

From the observation of the past, it is obvious that the development of future THz systems is closely related to the development of laser systems. The properties of the lasers significantly shape the specification of the THz systems. This paper therefore focusses on recent advances that are particularly relevant to take THz-TDS to real-world applications, that is an increase in their average power.

B. HIGH AVERAGE POWER SYSTEMS

Many efforts have been dedicated in the last decades to improve the performance of THz-TDS systems. From the emitter point of view most of these efforts have focused on increasing single pulse energy or bandwidth, typically at the expense of average power.

The average power of a THz pulsed source is by definition the product of the single pulse energy and the repetition rate and is the critical figure of merit for applications where signal-to-noise-power-ratio (SNR) or dynamic range are limiting. It is important to note that it is the combined performance of emitter and receiver that make a final solution possible; and many successful research efforts have been dedicated

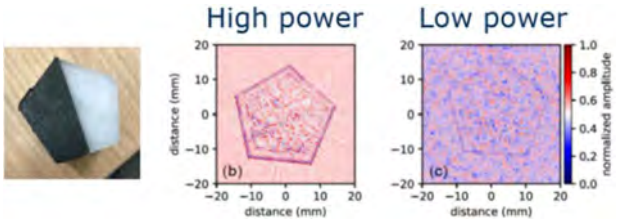

FIGURE 2. THz-time-of-flight 2D imaging in reflection of a 3D printed object (left image), comparing the image reconstructed using the same measurement time using a commercial low-power THz-TDS (200 μW average power) and a home-built setup (20 mW average power) in identical imaging situations. Higher average powers allow to reconstruct the object with significant better SNR. Figure adapted from [35].

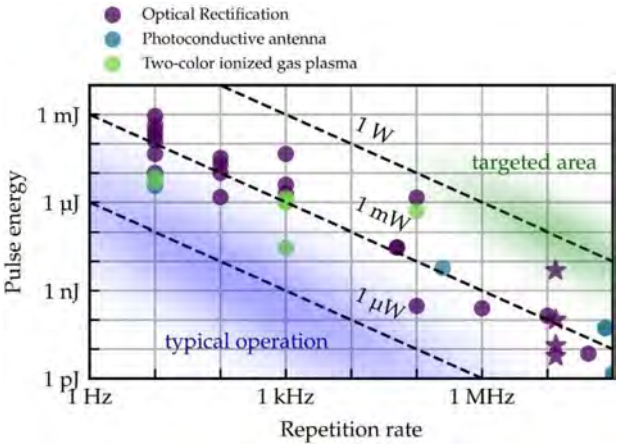

FIGURE 3. State-of-the-art of average power of lab-based THz-TDS sources, showing a selection of recent results aiming for achieving high average powers. Highlighted with stars are recent results achieved at high repetition rate >1 MHz using OR using high average power driving sources.

to improve the detection sensitivity, reaching record-holding values [33]. The combination of such sensitive detectors with higher average powers would enable new applications that could so far not be considered due to the current performance limits. Some examples of applications that benefit from an increase in average power of current THz-TDS are THz time-of-flight imaging in difficult scenarios, such as outdoors where air humidity attenuates THz frequencies strongly, or when observing reflected objects with strong scattering or low reflectivity, THz communications where traditionally only short-distance links are considered, or spectroscopy at remote distances. In Fig. 2(a), clear example in time-of-flight imaging is presented where high-average power THz-TDS can bring significant advances based on a lensless imaging approach [34].

The current state of the art of THz-TDS systems is illustrated in Fig. 3. As can be seen, most common TDS systems operate with THz average powers from the emitter <100 μW, making many real-world application scenarios difficult to implement in practice.

Of particular practical importance in THz-TDS systems is an increase in the average power of high-repetition rate

systems beyond megahertz. In fact, because many pulses are needed to reconstruct a single THz pulse, the acquisition time is ultimately limited by the repetition rate of the laser. Additionally, the extremely challenging scenarios addressed by these sources will additionally require averaging over many pulses, which can only be done in reasonable measurement times at very high repetition rate.

The low average power of current THz-TDS systems is intimately linked to the low average power of commonly used ultrafast lasers driving them; in fact two technologies are most commonly used in THz systems: Ti:Sapphire oscillators and amplifiers at 800 nm, mostly deployed in lab-based settings, and low-power ultrafast fiber lasers at telecommunication wavelengths of 1550 nm based on commercial THz-TDS. Both laser systems are limited to maximum average powers in the order of $<$1W. In combination with typical small conversion efficiencies $<<$1 %, this has clamped progress in the generation of higher average power THz-TDS.

However, driving ultrafast lasers have also in parallel made extremely large progress in terms of average power in the last decade, thus opening the door to much higher average power THz-TDS. Nowadays, femtosecond laser systems exceed the kilowatt average power level at around 1 μm with Yb-based gain media in improved cooling geometries [36], [37], [38]. These developments have opened the door to a rather new and forward-looking field of high average power, ultrafast laser-driven THz sources. Some noteworthy recent demonstrations include the demonstration of a 66 mW THz-TDS at 13.4 MHz repetition rate based on OR [39]; a 640 mW average power two-color plasma-based THz source at 500 kHz repetition rate [40] among several other recent demonstrations in this direction.

Next research directions in this field will most likely address high average powers in the multi-ten to multi-hundred mW average power at much higher repetition rates $>>$100 MHz; as well as combining this high average power with ultra-sensitive detectors for record high dynamic ranges and very short measurement times.

It is to be expected that such high average power systems will open up new application fields or make the community revisit old problems that were difficult to tackle. Some examples are given above, but some aspects of other fields considered very difficult could be revisited as well, for example the use of THz-TDS for biomedical applications. One critical factor to determine which application fields will be opened up by these new sources is the cost of the achievable systems, which will be determined by their adoption into the industrial landscape.

C. COMPACT SYSTEMS

A major aspect affecting the size and cost of a THz system is the light source used. As described previously, fiber lasers were an important step toward compact systems because they are intrinsically fiber-coupled and the gain medium is pumped through an electrically driven diode laser. The logical step to further miniaturization is the direct use of diode lasers to drive the THz spectrometer. Laser diodes have the advantage that they can be integrated monolithically, are electrically driven and have a footprint of less than 1 mm^2. Laser diodes are used in THz frequency domain spectroscopy (FDS) and THz-TDS systems.

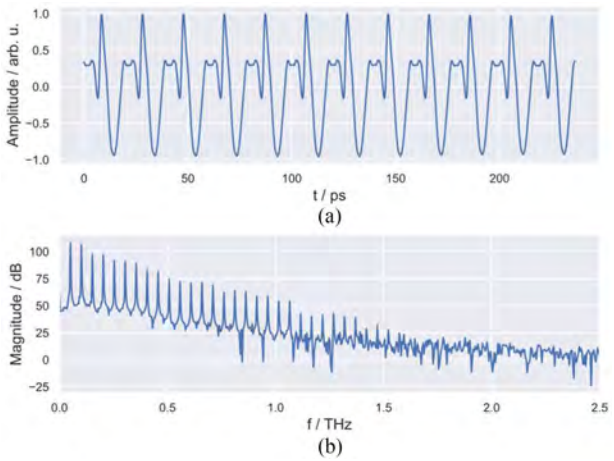

FIGURE 4. (a) Time-domain trace of an UHRR-THz-TDS system and (b) the corresponding frequency domain representation.

THZ-FDS systems are based on the superposition of two single frequency lasers. The superposition produces a beat signal at the difference frequency of the two lasers. This principle was first demonstrated in 1993 with two titanium:sapphire lasers [41]. Only 2 years later, a system based on laser diodes was presented [42]. This system concept is much more compact than THz-TDS systems. In addition, a frequency resolution that only depends on the accuracy in tuning of the two lasers is given. For example, a resolution of about 10 MHz was demonstrated [42]. In THz-TDS systems, on the other hand, the resolution is given by the length of the delay line and is typically in the range of a few GHz. A disadvantage of THz-FDS is the long measurement time. Combined with the high frequency resolution, measurement times of several 10 minutes are common. Liebermeister et al. presented a system which solves this issue and achieves a measurement time of 5 ms by using a fast tunable laser. By averaging, a DR of 117 dB with a bandwidth of 4 THz was demonstrated [43]. A comprehensive overview of THz-FDS systems and their applications is given by Preu et al. [44].

There are two approaches for THz-TDS type systems. First, simple multi-mode laser diodes (MMLD) were used to drive a conventional THz spectrometer. Since the light source is an incoherent source, this approach was called THz cross-correlation spectroscopy (THz-CCS) [45] and later became known as THz quasi time-domain spectroscopy (THz-QTDS) [46]. The second approach is to use a mode-locked laser diode (MLLD) and was demonstrated in 2017 [47]. This emits a pulse train which, corresponding to the short resonator length, has a high repetition rate. Because of the high repetition rate, these systems are referred to as ultra-high repetition rate (UHRR) THz-TDS [48]. Fig. 4 shows the time and frequency range. The repetition rate of 50 GHz of the laser is visible

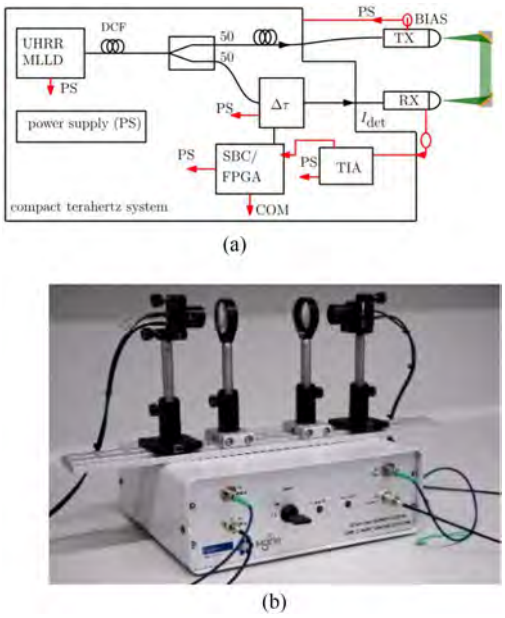

FIGURE 5. **(a) Schematic representation of the compact UHRR-THz-TDS system and (b) picture of the system.**

in the THz trace as well. The pulses have a spacing of 20 ps and this periodicity can be also seen in the frequency domain. It is notable that the peak dynamic range exceeds 120 dB and hence outperforms state of the art THz-TDS systems driven by fiber lasers in this regard. This increase in SNR was achieved in part by using a PIN-PD as the emitter instead of a photoconductor [49]. Similar performance can also be expected when using an uni-traveling-carrier (UTC) PD [50].

It should be noted here that signals from THz-CCS/QTDS systems exhibit the same periodicity when driven by laser diodes [51]. This is accompanied by a low frequency resolution. Therefore, these systems are not suitable for high-resolution spectroscopy. To overcome this problem, a superluminescent diode (SLD) can be used since it has a broadband unstructured spectrum. This approach was demonstrated for the first time in 2019 [52]. However, the continuous spectrum is accompanied by a reduction of the dynamic range [53].

However, the high repetition rate also has advantages when it comes to developing compact systems. Since the full information is contained in one period, a very short optical delay unit can be used. Fig. 5(a) shows the schematic for a compact, fiber-coupled, and MLLD driven THz-TDS system. The photocurrent at the receiver (Rx) is amplified by a transimpedance amplifier (TIA) and sampled by a combination of a single board computer (SBC) and field-programmable gate array (FGPA). All components except the THz path are housed in a 300 mm x 270 mm x 110 mm enclosure (see Fig. 5(b).

D. COMPARISION AND OUTLOOK

Competing technologies to THz-TDS and FDS are FTIR, electronic THz systems, and quantum cascade lasers (QCL). As described above, FTIR has the disadvantage that especially low frequencies (<1THz) can be reached only poorly and phase information is missing [54]. Electronic systems are limited both in terms of maximum bandwidth and central frequency [55]. With QCLs, there is also a difficulty to realize low frequencies as well as a high bandwidth. The frequency range is usually >1 THz and the bandwidth is limited to 1 decade [56]. In addition, cryogenic cooling is required.

Important tasks for the future will be to extend existing material databases to complete spectroscopic data over the whole available frequency range. Examples of these databases are high-resolution transmission molecular absorption database (HITRAN) [57] and Cologne database for molecular spectroscopy (CDMS) [58]. In the future, these databases will play an important role in the development of new devices and can also be used for material identification by using machine learning [59]. Especially for strongly absorbing samples, systems with a high SNR are needed here. Compact and cost-effective systems are, e.g., required to serve potential industrial applications [1] or for the examination and restoration of art objects and monuments [60].

Another important point for the competitiveness of THz-TDS systems is the increase of the measurement speed. Usually, multiple measurements are averaged to ensure a sufficient SNR. Accordingly, an increase in transmit power can be translated into a reduction in averaging. A direct increase of the measurement speed can be achieved by replacing the mechanical delay line by concepts like asynchronous optical sampling (ASOPS) [61] or electronically controlled optical sampling (ECOPS) [62]. Here, a high repetition rate of the lasers is particularly advantageous, since this reduces the demand on the sampling electronics. Examples from optical distance measurement can be directly applied to UHRR-THz-TDS systems where measurement speeds >1 MHz were realized [63], [64].

III. IMAGING SYSTEMS

A. IMAGING SYSTEMS FOR FREE FORMS

At the early stage of THz-TDS systems, the laser pulses were guided in free space. This made THz systems inflexible. THz time-domain spectrometers were set up on an optical table and thus non-portable. In 2000 the first fibre-coupled THz systems were introduced by Picometrix [65]. It allowed for a free movement of THz antennas and therefore provided flexibility. In 2007 a further advancement was demonstrated by Wilk et al. [66]. They presented a THz-TDS system based on a cost-effective fibre laser operating at a wavelength of 1.55 μm. Such systems comprise low-cost telecom components and are developed for long-term operation. The system was enabled by a new antenna material: low-temperature grown InGaAs/InAlAs multiple-quantum wells.

After this first demonstration this material system constantly improved over the years. This is illustrated in Fig. 6 which shows power spectra generated and detected with state-of-the-art PCAs from 2012 (orange) and 2021 (blue). The

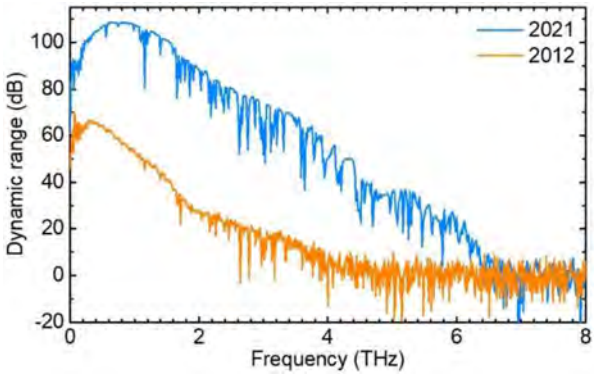

FIGURE 6. Comparison of power spectra generated and detected with state-of-the-art PCAs from 2012 (orange) and 2021 (blue). Spectra were recorded with a fiber coupled THz TDS system illuminated with femtosecond pulses centered around 1560 nm from the respective year.

orange curve corresponds to PCAs made of low-temperature grown (LTG) InGaAs/InAlAs multilayer heterostructures doped with beryllium (Be) [67] whereas the blue curve was measured with PCAs made of rhodium (Rh) doped InGaAs [68]. Note the bandwidth increase from approx. 3.5 THz (2012) to 6.5 THz (2021) and the >40 dB higher dynamic range of the 2021 spectrum. These improvements were mainly achieved by higher optical-to-THz conversion efficiency and improved material properties (lifetime, mobility, resistivity) of the PCAs. The latest antenna generation based on photoconductive membranes offer a bandwidth of up to 10 THz [69]. Hence, meanwhile THz systems comprising these antennas offer an excellent SNR and a bandwidth of several THz. Furthermore, these systems, which are commercially available from several companies, show an excellent long-term stability. Hence, measurement campaigns over several days [70] or even weeks [71] are feasible.

The acquisition of THz images usually takes only a few minutes and at most a few hours. The first images with a THz TDS system were taken at Bell Laboratories in 1995 [30]. This involved moving the mostly flat samples through an intermediate focus in a raster pattern. The transmitted THz pulses were analyzed for each pixel, so that an image was formed step by step.

Since that time, many different flavors of THz imaging have been demonstrated (see [72] for a review). One variant is THz tomography, in which objects are scanned in reflection [73], [74], [75]. Analogous to ultrasound examination, THz tomography obtains a series of reflections originating from the different interfaces in a sample. Unlike ultrasound measurements, THz technology uses transverse electromagnetic waves rather than longitudinal sound waves. One advantage over ultrasound is that the probe does not have to touch the sample but is positioned at some distance. In any case the internal structure of the objects can be concluded from the pattern of the reflected THz pulses.

Early THz tomography systems had a stationary focus through which a sample was moved in a two-dimensional

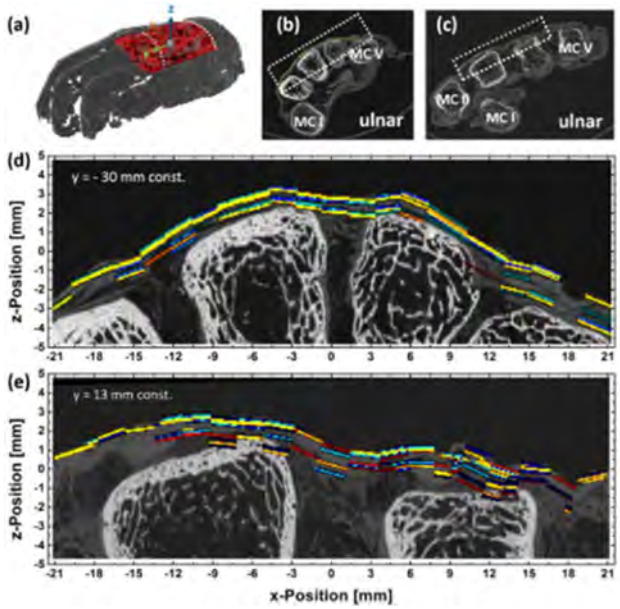

FIGURE 7. Comparison of layers reconstructed from the THz measurement and a micro-CT scan. (a) shows the determined 3D shape of the hand. The red area indicates the region investigated with THz tomography. (b) and (c) show cross-sections along the white dotted lines in part (a). (d) and (e) show magnifications of these cross sections. The colored lines indicate layers identified in the THz scan. The figure is reproduced from [77] within Creative Commons CC BY license.

grid pattern to obtain an image. To obtain such images it is important that the sample is always in the focus and that the direction of incidence is parallel to the surface normal. Hence, only flat, i.e., planar samples could be measured, which significantly limited the sample selection.

Recently, Stübling and coworkers attached a fibre-coupled THz system to a robotic arm and such demonstrated a system that enables spectroscopic and imaging THz measurements on free-form objects [76]. With this system, the THz emitter and receiver can be positioned perpendicular and at defined distance to the sample surface for each pixel. First the outer shape of the object is determined using a commercially available fringe projection system. One task is to connect the 3D scanner coordinate system with the robot or real-world coordinate system, respectively. This requires additional scans of a known reference pattern. More details on the system can be found in [76]. Using this system Stübling et al. studied an ancient mummified human hand [77].

The results are shown in Fig. 7. It shows a 3D shape of the hand (part a) and four images taken by micro computed tomography (μCT). As compared to conventional CT, μCT provides a better spatial resolution. Yet, the sample size is limited; a full human body or an entire mummy cannot be investigated. Fig. 7(b) and (c) show cross sections through the hand along the dashed lines shown in Fig. 7(a). Fig. 7(d) and (e) display magnifications of these images; the magnified areas are indicated by the dashed boxes in Fig. 7(c) and (d). The colored lines in Fig. 7(d) and (e) indicate the layers which have been found using THz tomography (see [77]) for

more details. These results agree well with the μCT. The results suggest that THz tomography imaging offers better depth resolution than conventional CT. The depth resolution is comparable to that of a micro-CT scan. Furthermore, THz measurements using the developed system have the advantage over μCT that comparably large samples can be scanned, which would not fit into a conventional μCT device.

In addition, such a system was recently used to study the sub-surface structure of a wooden putto (wood carving of an infant) [78]. Delaminations of polychrome and preparation layers as well as damages on the wooden substrate due to insect tunneling could be detected. Hence, this technique enables the restorer to find hidden damages of the object that cannot be seen by visual inspection only. This is important as the climate changes and extreme temperatures lead to increased anobial infestation and mold growth in exposed sacred wood objects, which significantly reduce the wood's strength.

Thus, in the future, simple, easily portable "hand-held devices" must be developed, which restorers and monument conservators can use on site according to restoration standards. Then it should be possible for the first time to evaluate and monitor the strength of bound cultural objects made of different types of wood in situ in a reproducible and digitized manner, without destroying or touching them. In particular, the high SNR of THz-TDS systems of more than 100 dB will be beneficial. The increase in SNR is closely related to the advancement in PCAs [79].

Overall, it can be expected that the technique of THz tomography will become more widespread in non-destructive testing, for example, to determine the thickness of tablet coatings [80] or of paint layers [81], [82], [83]. This area will benefit greatly from the development of compact systems as described in the previous section.

B. INTEGRATED NEARFIELD IMAGING SYSTEMS

A far-field THz imaging system has a significant distance between the optical elements and the object, which results in about a half-wavelength resolution, which is in the millimeter range at THz frequencies [84]. Near-field imaging is essential for analyzing localized electromagnetic properties at microscopic or nanoscopic scales, demonstrating its importance.

In general, THz near-field probing methods fall into two categories. The first method uses a THz-Near-field Scanning Optic Microscope (NSOM) system to measure evanescent waves emitted as a result of scattering due to sub-wavelength objects [85]. These methods are prevalent for nanoscopic imaging in the THz range. However, NSOM systems have a high system cost and low integration level that limit their use to laboratory environments and fundamental science fields. The second method uses "Active" probing where a near-field probe is brought in proximity to the sample, changing its energy distribution and stored energy according to the sample's dielectric properties. Subwavelength antennas such as small dipoles, open-ended waveguides, or other geometries can be used for these probes [86]. A major drawback of all these THz platforms is their high costs, low integration, and poor reliability when deploying in mass. As a result, THz applications require single-chip solutions that do not require complex microelectronic assembly.

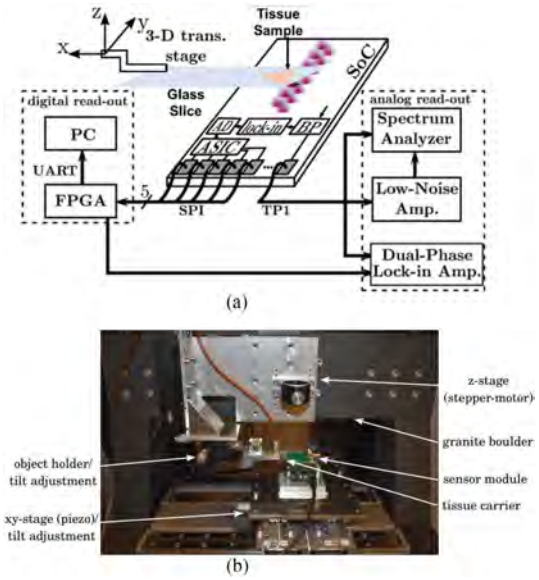

FIGURE 8. **(a) Diagrammatic representation of characterization setup of the SoC [90]. An excised tissue sample is placed between two glass slides and is positioned above the sensing surface for the characterization of the sensor response. (b) Measurement setup for the tissue scan.**

Initial demonstrations of nanoscale silicon-based THz imaging devices have overcome some of the above-mentioned drawbacks by enhancing sensitivity and integration levels [87], [88]. More particularly, related advances were enabled by cointegrating the Split Ring Resonator (SRR) subwavelength near-field probe, a THz illumination source, and a THz detector on the same silicon die into a single sensing pixel [87], [89]. This technology was further used for the development of a fully integrated 128-pixel System-on-a-Chip (SoC) based on the capacitive interaction between on-chip split-ring resonators (SRRs) to deliver real-time super-resolution near field imaging of around 10 μm at 550 GHz [90]. This SoC was integrated on a chip scale using a parallel sensor excitation scheme using 4-way power division networks and a rolling-shutter sensor readout architecture utilizing on-chip lock-in detection.

The presented SoC offers a complete set of functionalities, including THz near-field sensing, analog signal conditioning, analog-to-digital conversion, and a digital communication interface. This SoC is also capable of acquiring rapid images of several mm^2 objects, which require only a conventional USB port to work as a standalone device [90]. Specifically, the use of this SoC for imaging excised breast tissue was demonstrated as illustrated in Fig. 8(a) and (b). The analog readouts were measured at the test point (TP1) and the digital readouts were measured using on-chip lock-in amplification (LIA) and analog-to-digital conversions. In Fig. 8(b) a picture of the experimental setup can be seen.

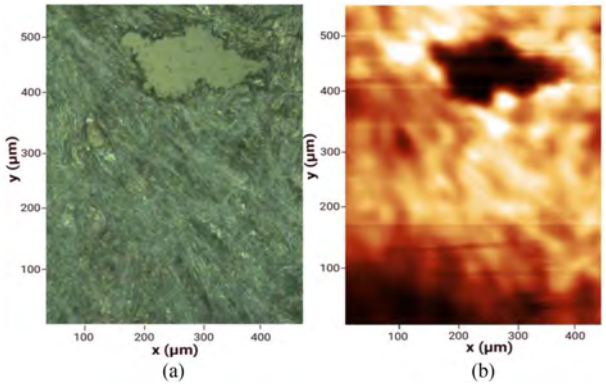

FIGURE 9. (a) Micrograph and (b) THz near field image of excised breast tissue. The raster scanning was done with 100 ms of step time.

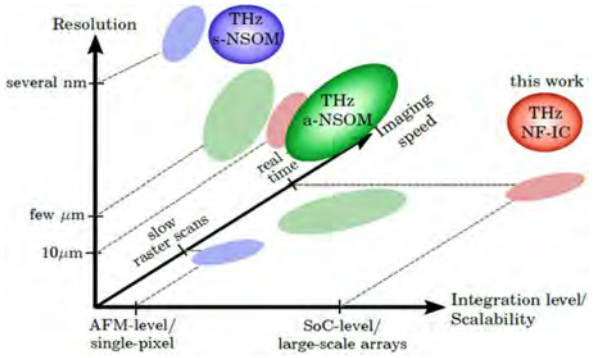

FIGURE 10. Illustrative comparison between the THz near-field sensor IC [90] and contemporary THz near-field technology.

Fig. 9(a) depicts an imaging result of the excised tissue obtained from histopathology. Fig. 9(b) shows the image from the proposed near field imaging setup. The image clearly exhibits sufficiently high contrast and resolution to facilitate microscopic feature extraction.

Fig. 10 shows a qualitative comparison of the presented near-field imager with conventional THz NSOM methods. The proposed on-chip cointegration mitigates remote illumination and detection sensitivity problems in THz NSOM. Multi-pixel integration on a chip-scale further enables real-time, microscopic, THz imaging within seconds using unprecedented SNR.

Design challenges remain with large-scale integration of near-field 2D sensors. The 1D pixel geometry of the THz front-end presents significant spatial under-sampling due to the size of the oscillators and power distribution networks employed. Thus, new design methodologies and sensing concepts are required for 2D sensor integration.

IV. BEAM STEERING SYSTEMS

A beam steering system is capable of directing waves from a fixed source (or detector) to a target arbitrarily located within range. This technology is critical for THz waves that propagate in line of sight. Beam steering for THz wireless communications is associated with directive radiation to counterbalance relatively low source power and high free-space path loss and therefore maximize SNR at the receiver. In the case of radar imaging with a single transceiver, beam steering is a part of near-field focusing that aims to enhance image resolution for stand-off detection. A key to beamforming is to craft a suitable spatial phase response on a transmitting surface, while beam steering requires dynamic alteration of this phase response within 360 degrees with some tuning mechanism. A number of tuning mechanisms have been considered for THz beam steering. These include micro-electro-mechanical systems (MEMS), phase change materials, liquid crystals among others. The pros and cons of these tuning mechanisms have been discussed in a review paper [91]. An overview of beamsteering techniques is also given in [92] focusing on the application of metasurfaces. A review of beamforming techniques for ultra-massive MIMO communications is presented in [93].

While beam steering is prevalent in the neighboring microwave and optical ranges, it is not possible to directly scale these existing techniques to the THz range. Here, three common approaches for beam steering implemented in the THz regime are discussed with some recent and representative realizations. Considerations are placed on efficiency and bandwidth that are most critical to THz applications. Bandwidth in direct proportion to depth or axial resolution in sensing, while supporting high data rate in communications. Other secondary factors of interest include steering angular range, steering speed, integrability, and structural complexity.

A. PHASED ARRAYS

The concept of a phased array has been long implemented in RADAR and more recently in LiDAR systems. In brief, an array of sources (or receivers) on a distributed network is equipped with an equal number of phase shifters to control the phase profile of the radiated waves. While phase shifters are available in the microwave and optical domains based on different technologies, there appears no counterparts that are as effective in the THz domain. Typically, varactor diodes are used in microwave and millimeter-wave phase shifters to vary distributed capacitance along a transmission line and therefore change the propagation constant. THz varactor diodes exist by scaling down the cross section of microwave varactors so as to reduce the overall capacitance. However, this practice gives rise to excessive parasitic ohmic loss, and the loss is further exacerbated by strong wave confinement in metallic transmission lines. In optics, beam steering is conducted via the electro-optic or the thermo-optic effect. The former is by changing the refractive index of a guiding element by an applied electric field, known as the Pockels effect. The latter alters the index by a heating element. However, it is not possible to inherit the same effects in the THz domain since the amount of phase shift scales with frequency, i.e., THz waves see much smaller phase shifts. Nevertheless, these technological roadblocks have been circumvented by different ingenious techniques. One approach is to decentralize the source into an

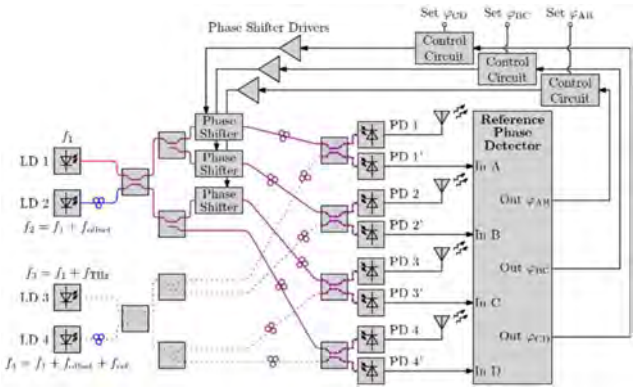

FIGURE 11. Phase control concept for a photonically steered THz phased array transmitter according to [99].

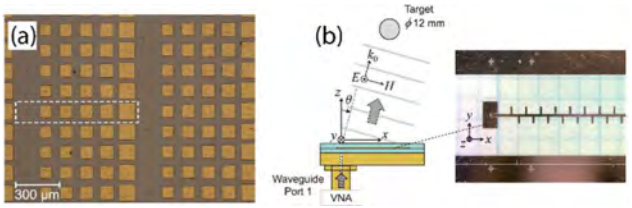

FIGURE 12. Planar scanning system. (a) Reflectarray exhibiting beam squint around 1 THz [104]. (b) Slow-wave LWA performing spatial scanning by means of beam squint [105].

array of oscillators collocated and codesigned with radiating elements, and controlling an oscillator condition results in a desirable phase profile. This technique was used in a SiGe BiCMOS realization at 340 GHz [94], for instance. While the approach is effective, the circuit complexity increases significantly, limiting large-array implementations. Another approach used a sparse array to reduce the complexity of electronic phase shifting, where grating lobes in the radiation pattern are subdued by the narrow beam of an auxiliary lens array [95].

Especially on the transmit side, a further possibility to realize a phased array or even a beamformer is based on optoelectronic generation of THz signals. By heterodyne detection (mixing two optical signals at a photodiode) a difference frequency signal at THz frequencies can be generated. The output current of the photodiode or photoconductive element then directly feeds the transmitting THz antenna. In this concept, phase-shifting and modulation of one of the optical signals is directly converted to the generated THz signal with the same amount of phase shift. As already mentioned, utilizing the electro-optical or thermo-optical effect, the phase of one of the optical signals can easily be shifted - and by a combination of couplers and phase shifters (Mach-Zehnder modulator) also the amplitude can be modulated. The optoelectronic approach has the advantage that the power of multiple THz transmitters can be combined to increase the power density into a certain direction. The optoelectronic approach can be applied for both concepts, beam steering and beam forming.

An early experiment of photonic beamforming at 85 GHz has been presented in [96]. Different photonic beamforming concepts have been analyzed theoretically with respect to their power budget [97]. An overview of optoelectronically assisted beamforming including an integrated optical beamforming network (OBFN) chip has been given in [98]. Even in an integrated photonic circuit, phase drift of optical waves cannot be completely avoided, but can be compensated by a phase control concept [99], see Fig. 11. Using four laser diodes, THz signals with frequency f_{THz} as well as a microwave signals with frequency f_{ref} are created. It can be shown that in this four antenna beam steering system, the THz signals and the microwave signals have the same phase relations so that the microwave signals can be used for phase control of the THz transmit signal.

B. BEAM STEERING WITH PLANAR AND PASSIVE SYSTEMS

Beam steering can be conducted by planar and passive components including the groups of reflectarrays, transmitarrays, and leaky-wave antennas (LWAs). In nearly all these cases, there are no active tuning components, and steering relies on frequency-to-angular mapping or beam squint as a result of fixed phase shift with respect to frequency. Consequently, the bandwidth becomes dependent on distance. By sweeping frequency, the beam direction can vary to scan a target, mostly in one direction. However, the relatively small bandwidth of these concepts significantly reduces the achievable radial position resolution of radar systems. Benefits of these platforms lie in simplicity and efficiency, and they can be retrofittable to a wide range of sources and detectors.

Specifically, the groups of reflectarrays and transmitarrays with their long history in the microwave domain are known in the modern context as metasurfaces [100]. These passive arrays are fed from free space by a source located in proximity, and as such compromising compactness. Every subwavelength element on the surface, as shown in Fig. 12(a), collectively imposes a pre-designed phase profile to form an outgoing beam in reflection or transmission for a reflectarray or a transmitarray, respectively. While the two types of arrays are closely related, transmitarrays are more integrable to portable systems due to direct alignment with antennas. In any case, the main origin of the losses is from a dielectric material used to support the array [100]. To mitigate the issue, cyclo-olefin copolymer (COC) that has exceptional low loss for THz waves has been used in fabrication of these arrays [101]. The concept of passive arrays have received renewed interest in the form of ‘reconfigurable intelligent surfaces (RIS) [102] to perform active beam steering for 6G communications. A prominent example is a reconfigurable transmitarray operated at 300 GHz [103]. This CMOS-based array can reconfigure its scattering element to achieve phase variation of 360 degrees, sufficient to form different beam patterns.

Reflectarrays can also be based on MEMS which are used to control the position of a large number of small mirrors. A well-known concept for the positions is that of a periodic

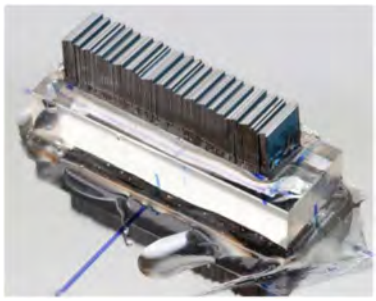

FIGURE 13. Mock-up of an adjustable reflectarray with 80 static reflectors of dimensions 300 μm x 5000 μm with optimized mirror positions according to [106].

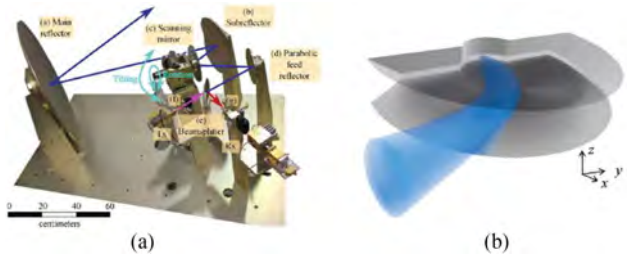

FIGURE 14. Mechanical scanning systems. (a) Gregorian optics for body scanning at 300 GHz [111]. A mirror moved in two axes for beam steering. (b) Parallel-waveguide-enabled Luneburg lens at 300 GHz. 1D beam steering was achieved by titling one plate [112].

blazed grating with sawtooth-shaped mirror positions where the approximate specular reflection coincides with the first order diffraction maximum. It has the advantage of creating high gain into the desired direction but suffers from large grating sidelobes of the beam pattern. In [106] it could be shown that sidelobes can be avoided by optimizing all mirror positions by a suitable optimization algorithm. The resulting optimum mirror positions are not periodic anymore and show only locally a sawtooth-shaped distribution, see Fig. 13.

On the other hand, LWAs are more integrated since they are in the form of waveguides directly coupled to a source or detector. Both slow-wave and fast-wave LWAs have been implemented at THz frequencies, mostly through microstrip lines and parallel-plate waveguides, respectively. Its beam scanning enabled by frequency sweeping was used to demonstrate radar imaging with an example structure shown in Fig. 12(b) [105], [107]. Some other demonstrations used such THz LWAs for wireless communications [108], [109], but this encountered angle-dependent frequency & bandwidth use. One demonstration creatively used a fast-wave LWA for frequency (de)multiplexing in THz wireless communications [110]. In this case, a parallel-plate waveguide combined, guided, and separated two carrier frequencies with an aggregate data rate of 50 Gbit/s.

C. MECHANICAL SCANNING SYSTEMS

Mechanical beam scanning is a popular and diverse in technique for THz beam steering. It involves moving elements such as step motors or piezoelectric materials to manipulate a THz beam. With mechanical movement, indeed the scanning speed is expectedly conservative, around kilohertz at best, but this serves the purposes for both communications to track a receiver and radar imaging to raster-scan a target. Most realizations involve reflective or transmissive optics that provide true time delay and as such truly broadband. While the technique is apparently straightforward, precise control of the moving mechanics is a challenge in light of THz wavelengths in the sub-millimeter range. Among a great deal of realizations, here some representative ones are discussed. One early implementation shown in Fig. 14(a) involved a Gregorian reflector system for active imaging via frequency-modulated continuous-wave (FMCW) radar at around 300 GHz [111]. In that reflector chain, one flat mirror enabled target scanning via its two axes of movement and achieved 2 frames per second for a whole human body at 8 meters away.

Another 300 GHz FMCW body scanning system from RIKEN exploited human walking to scan across the body, while vertical scanning was by means of a Galvano scanner [113]. Some recent implementations were based on optical techniques involving lenses or prisms. The former case used a Gimbal mirror for two axes of scanning in coordination with a telecentric f-θ lens that focuses an oblique incident beam onto a target at normal incidence [114]. In the other case, Risley prisms were 3D-printed to operate at around 300 GHz [115]. The output Bessel beam was steered in both azimuthal and elevation axes by rotating the two prisms. The bandwidth was limited due to phase wrapping to reduce material loss in those prisms. An unconventional case in Fig. 14(b) involved a Luneburg lens made of a parallel-plate waveguide with spatially varying separation to control local modal index of the TE_1 mode around 300 GHz [112]. Tilting of one plate resulted in beam deflection in 1D with a bandwidth $>$20 GHz, limited by the dispersion and mode cutoff.

D. COMPARISION AND OUTLOOK

Up to this point, multiple techniques applicable to beamsteering for terahertz waves have been discussed. They are either drawn from microwave techniques or optics with pros and cons. Phased arrays are prominent in their integrability, while transmitarrays, reflectarrays, and LWAs are simple and with large aperture. Mechanical steering comes with superb bandwidth and efficiency with drawbacks in integrability and speed. Table 1 summarizes prominent features of these techniques. Nonetheless, it is arguable to judge an all-rounded winner, which depends very much on the task at hand. At this point in time, beamsteering for terahertz waves is relatively new and there is room for improvement in all these techniques with a prime focus in efficiency and bandwidth. Especially phased arrays and similar approaches with their potential of being highly integrated and the advantage that multiple terahertz sources increase the output power exhibit long-term advantages.

TABLE 1. Comparison of Beamsteering Techniques. This Comparison Is Generic and Does Not Capture Outliers That May Perform Better or Worse in Some Factors

	Phased arrays	Transmitarrays & reflectarrays	Leaky-wave antennas	Mechanical steering
Efficiency	Low-medium	High	Medium-high	Very high
Bandwidth	Medium	Low	Low	Very high
Speed	Very high	Medium-high	High	Low
Integrability	Very high	Low	High	Low
Complexity	Very high	Medium	Medium	Low
Aperture size	Small	Large	Medium	Very large
Retrofittability	Not possible	Yes	Yes	Yes

V. COMMUNICATION SYSTEMS

First ideas on THz communications, covering the spectrum range beyond 100 GHz, have been published between 2007 and 2011 [112], [116], [117]. Due to the large amount of available spectrum –especially beyond 275 GHz – it is possible to achieve data rates of 100 Gbit/s and beyond with transmission systems of moderate spectral efficiencies. A major drawback of these high frequencies is the high path loss, which must be mitigated by using high-gain antennas in combination with line-of-sight (LOS) or obstructed line-of-sight (OLOS). In OLOS a communication link is established via a single reflection or scattering process. Challenges coming with high-gain antennas are amongst others the device discovery during link set-up and the beam-tracking in case of at least one mobile transceiver. The frequency range of interest also covers the so-called THz gap, where both electronic and photonic approaches are suffering from (the same) low output powers when generating the THz signals. On the other hand this allows also two principal approaches to generate THz signals. Hence, from the very beginning of developing THz communication systems, the scientific community have worked towards the realization of both photonic [118] and electronic [119] transmitters.

A. STANDARDISATION AND REGULATION

In the most recent years THz communications has been no longer a pure research topic but has reached already standardization bodies. In 2017 IEEE Std 802.15.3d, the first wireless standard operating in the frequency range 252-325 GHz, has been published by IEEE 802 [120]. This first standard assumes fixed point-to-point links covering applications like intra-device communication, kiosk down loading, wireless links in data centers and backhaul/fronthaul links [121]. All these applications have in common, that the positions of the high-gain antennas at both ends of the link are known avoiding complex device discovery and beam tracking procedures. Nowadays THz communications is seen as a potential candidate for one of the PHY layers in the 6th generation of wireless communication systems. For example, the 6G flagship project mentions in its white paper [122] that THz communications is an enabler to achieve wireless data rates of 1 Tbps. This may trigger future standardization activities at the 3rd Generation Partnership Project (3GPP).

In 2019 the world radiocommunication conference (WRC 19) has identified 137 GHz spectrum in the frequency range between 275 and 450 GHz for mobile and fixed service [123], [124]. This was enabled by intense sharing studies with passive services like earth exploration satellite service and radio astronomy proceeding WRC 19. Together with the already allocated 23 GHz between 252 and 275 GHz a total of 160 GHz of spectrum is now available for THz communications between 252 and 450 GHz.

B. FWA DEMONSTRATIONS

In the last decade various hardware demonstrators have proven the feasibility of THz communication systems [119], [125], [126], [127], [128]. This non-exhaustive list includes a world's first demonstrations of a wireless transmission of 100 Gbit/s over 100 m using a hybrid photonic/electronic approach [125], a testbed with an antenna array for electronic beam steering [126] and an outdoor transmission for backhaul applications [127]. Recently, Samsung and University of California have presented an end-to-end 6G THz wireless platform with adaptive transmit and receive beamforming at a carrier frequency of 135 GHz [129]. LG and Fraunhofer HHI have successfully tested wireless transmission and reception at a frequency range of 155 to 175 GHz over a distance of 320 meters outdoors [130]. Most of these early demonstrators are based on the more expensive III-V technology, but also systems based on SiGe [128] and CMOS [131] have been successfully demonstrated.

While the hardware demonstrators mentioned above are all based on laboratory equipment like arbitrary waveform generators (AWG) and fast digital oscilloscopes to generate and receive the signal, the Horizon 2020 EU-Japan project ThoR has successfully demonstrated a 300 GHz bi-directional wireless backhaul link. With the ThoR link real data with a net data rate of 2 x 20 Gbit/s connecting two buildings separated by 160m, see Fig. 15, using a bandwidth of 8.64 GHz has been successfully demonstrated [132]. The ThoR solution is based on a super-heterodyne approach and provides a quasi-compliant solution with IEEE Std 802.15.3d-2017 [133], [134].

C. MOBILE 6G THZ COMMUNICATIONS

The deployment of 5G has been an exciting moment for operators across the globe to enhance their services and offerings.

FIGURE 15. 300 GHz ThoR link connecting two buildings at the campus of TU Braunschweig.

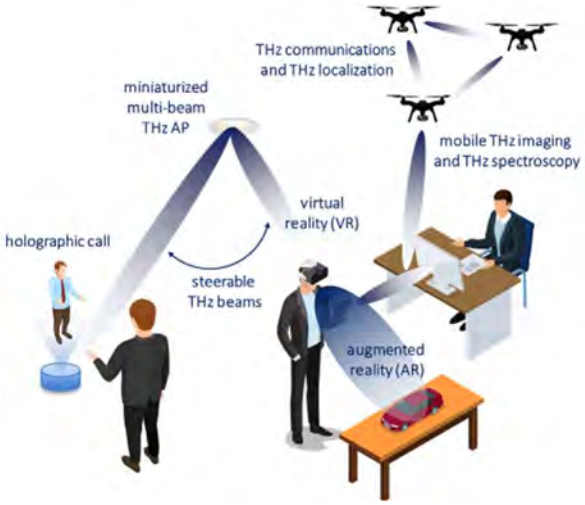

FIGURE 16. Potential short-range 6G use cases.

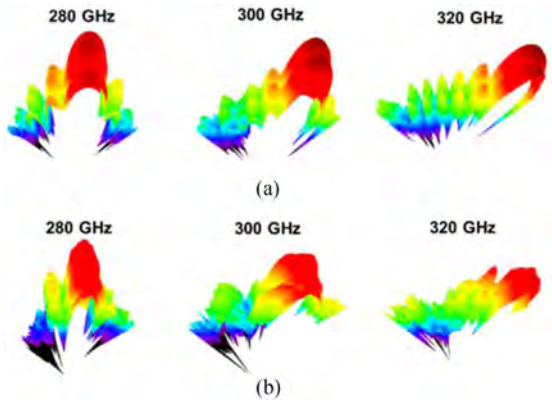

FIGURE 17. Simulated (a) and measured (b) far field THz radiation patterns using a beam steering antenna fabricated at University Duisburg-Essen [108].

While many operators first rolled out non-standalone (NSA) 5G (3GPP Release 15) [135], which basically employs the 5G new radio (NR) radio access network (RAN) overlaid on an existing 4G LTE network core [136], the deployment of standalone 5G (SA 5G) is now at focus. This will allow operators to fully exploit all the benefits 5G offers. Nevertheless, despite this success, 6G has already kicked-off and one of the candidate technologies for a 6G radio access technology (RAT) is THz communications, which uses spectrum mainly beyond 275 GHz as discussed in Section V-A.

This would open the use of channel bandwidths of several 10s of GHz for eventually reaching cell capacities exceeding 100 Gbit/s. Among other aspects, mobile 6G THz technology requires multi-beam steering and tracking to serve multiple users as shown in Fig. 16.

A key research challenge in this regard is the invention of highly integrated, steerable directive THz antennas to overcome the high free-space THz path loss. Consequently, several THz beam steering concepts have been proposed and studied [136]. Among them are conventional approaches including mechanical scanning technology [137], MEMS technology [138], and multi-feed switching [139]. Electrical phased-array technology is a well-developed solution to achieve beam steering at microwave frequencies [140] but when operating at THz frequencies, the high losses of semiconductor switches and other constrains limit its applicability. Therefore, alternative solutions were studied to overcome this drawback by modifying the phase before the frequency is converted to THz waves. A promising solution in that context which also could provide reasonable signal bandwidths for high data-rate THz communications are optical phase shifter [141]. For chip-integrated electronics, the perhaps most common and reliable approach is using CMOS based beamforming transceivers due to their scalability and cost [129], [142]. To reach longer wireless distances, the use of InP power amplifiers (PA) also may prove beneficial [143]. In [142], a 140 GHz over-the-air link supporting 16 Gbps over 30 cm was achieved using a CMOS chip with on-chip antennas. The chip enabled 1-D beam steering with a steering angle of $\pm 30°$. In 2022 Samsung reported 22 nm CMOS transmitter (with an InP PA for longer distance) and receiver RFICs at 135 GHz for an end-to-end 6G THz platform [129]. In this work, adaptive beamforming for 6.3 Gbps at 30 meter and 2.3 Gbps at 120 meter wireless distance was successfully demonstrated.

An alternative approach which benefits from its simplicity is to exploit frequency-scanning antenna such as leaky-wave antennas (LWA) for 6G THz communications. In a THz LWA, the phase shift between the array elements with a fixed interelement spacing is usually provided by changing the THz carrier frequency as shown in Fig. 17. This concept requires frequency tunable THz oscillators and frequency-independent THz receiver. In [144], [145], [146], optical heterodyning is employed for frequency-tunable THz generation and frequency independent single-chip Schottky barrier diode (SBD) detectors in combination with an IF modulation scheme for separating in-phase and quadrature components.

Here, 100 Gbit/s wireless transmission with spectral efficiencies reaching 9 bit/s/Hz (512-QAM-OFDM) is demonstrated for the 60 GHz ISM band. In [147], 100 Gbit/s wireless

THz transmission is demonstrated at 300 GHz using an analog bandwidth of only 12.5 GHz. By using a photodiode excited planar InP-based on-chip THz LWA, mobile THz communications is demonstrated for the first time in [148]. For single user operation, a minimum data rate of 24 Gbit/s is achieved within the antenna's scanning range of 33°. The scanning speed of 28°/s allows to steer the THz beam over the full scanning range within less than 1.2 seconds. Also, multi-user operation is theoretically studied, showing that up to 12 users with a total capacity of 48 Gbps can be supported.

D. FUTURE DEVELOPMENTS

Future development will focus on applications with strong mobility involved, e.g., trains [149] or cars [150] requiring significant scientific progress on device discovery, 2D THz beam steering and beam tracking. Automotive applications include both communication and radar systems. For the latter the frequency range beyond 300 GHz is also of interest due to the large available bandwidths enabling a high resolution. Such a combined radar/communication application may be part of future Joint Communication and Sensing (JCS) [151] concepts in 6G.

VI. LOCALIZATION SYSTEMS

Accurate indoor localization based on asynchronous and low-complexity infrastructure has recently gained great prominence for smart-world emerging applications like simultaneous localization and mapping (SLAM) systems and synthetic aperture radar (SAR) [151], [152], [153]. As an example, sub-mm accuracy localization is required for SAR applications in order to realize indoor room profiling with sub-mm resolution [154], [155]**.** Recalling Cramér–Rao bound, sub-mm localization accuracy could be achieved using the huge offered bandwidth at THz band [156], which is not available at other frequency bands.

In this regard, chipless radio frequency identification (RFID) systems [157] acting as a low-complexity infrastructure has been widely considered in indoor localization systems, as presented in [158]. From another point of view, the THz band becomes a key enabler for localization aided applications, since it provides localization systems with a superior time-resolution leading to high accuracy location estimation [159], [160]. The fusion of the THz band along with chipless RFID localization systems is proposed in [161] to achieve high-accuracy self-localization in indoor environments based on an unsynchronized passive and hence energy-autonomous infrastructure.

A. UNSYNCHRONIZED LOW COMPLEXITY INFRASTRUCTURE

Passive and chipless tags to act as anchors are considered as infrastructure for indoor self-localization systems [161], [162]. These tags are considered energy-autonomous infrastructure since the energy of the tags is drawn from the incident signals from the reader without a need for external power source (or battery) to operate.

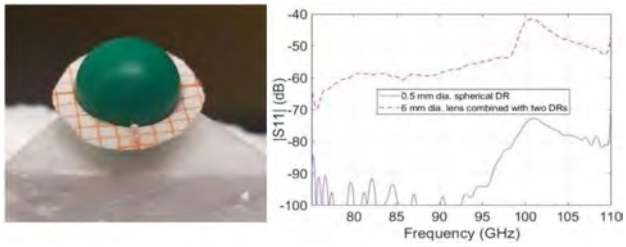

FIGURE 18. Combination of a dielectric lens (6 mm dia. from Polyamid) with two DR of 0.5 mm diameter glued (product name UHU POR) to a paper-ring around the lens with measured RCS spectral signature compared to signature of single DR; DUTs placed in 36 cm distance to horn antenna.

Many solutions to tag design at mm-wave and THz bands are proposed in the literature [161], [162], [163], [164], [165], [166] in order to mainly improve the coding capacity, the tag retro-directivity, and/or clutter suppression capability [163]. In this regards, different coding particles are combined with different retroreflectors (like lenses and corner reflectors) to achieve high retro-directive tags, while different coding particles are used like dielectric resonators (DR), frequency selective surfaces (FSS), and photonic crystals. For clutter suppression, many techniques are employed like twisting the polarization as proposed in [167]. In the following some examples of combining the DR as a coding particle with different retro-reflectors are shown.

Combinations between DR and a dielectric lens are proposed in [161], [163], [164], [165] to boost the radar cross section (RCS) of the chipless tag and attain a wide-retrodirective angle. In these combinations, the interrogator incident signals from the reader are collected by the lens aperture and concentrated into a DR, that is placed at the focal area behind the lens surface acting as a receiving antenna. Consequentially, the resonant modes of the DR are excited proportionally to lens antenna gain, and then the DR reflects the incident signal through the mode radiation patterns which couples part of the signal back into the lens, providing gain as in a transmit lens antenna [163], [164]. Fig. 18 presents a realized DR-lens combination with the measured reflection coefficient S_{11}. It is clearly noted that the RCS resonance peak, i.e., proportional to S_{11}, increased by about 30 dB over the response compared to a single spherical DR [163].

The design in Fig. 18 can be further improved by locating more DRs along the focal circle in order to extend the DR-lend combination coverage over a wide range of incident angle as proposed in [161], [163], [165]. Moreover, larger spherical Luneburg lenses is proposed in [168] to gain higher RCS.

An attractive alternative design is to attach a DR array to a trihedral corner reflector surface as shown in Fig. 19, where a planar array of DRs with a triangular shape is attached to a triangular opening of the corner reflector [163], [166]. The tag ID is observed as a notch, instead of a peak, in the broadband high-level RCS signature of the metal reflectors. This behavior results due to the scattering by the DRs and not absorption.

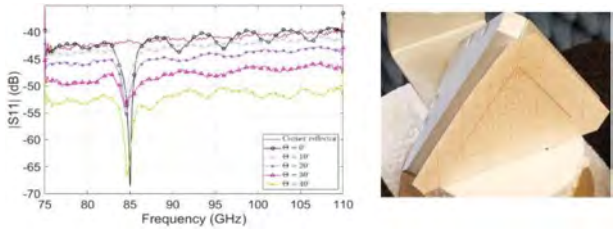

FIGURE 19. Trihedral corner reflector of 68mm edge length with planar array of 158 DRs of 0.6 mm diameter in a 2.5 mm grid fixed to the corner reflector aperture. Measured RCS spectral signatures for incident angle from 0° to 40° with signature of the reflector without DR array (full line) for comparison; DUT placed in 2 m distance to horn antenna.

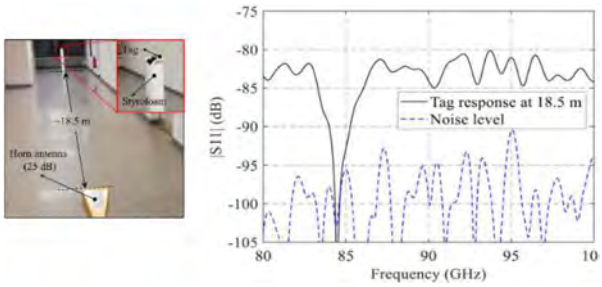

FIGURE 20. Measurements setup and magnitude of measured S11 in dB for long reading range compared to the noise level achieved by the VNA.

This design produces high RCS over a wide range of incidence angle and provides clear identification by the notch position in its spectral signature. The presented tags can be realized at higher THz frequencies by reducing the size of the DRs. Reducing the size would lead to challenges in fabrication which can be encountered either by using high-resolution 3D printing [169] or by using photonic crystals that are easier to realize at those frequencies [170].

Apart from innovating RFID tags that are originally used for indoor self-localization systems presented here, there is an increasing interest in building THz tags for the so-called THz identification (THID). THID is still in the early research stages where few numbers of THz tags are reported in the literature. In [171], the authors demonstrate a 1D photonic crystal resonator as the first THz tag where the coding is performed in volume instead of the surface. In [172], spatial and frequency coding is realized using a 2D PhC resonator. Very recently, the smallest THz tag was proposed in [173] based on CMOS technology. In addition, barcode identification systems are developed for the THz region as in [174], [175].

B. RFID BASED INDOOR THZ SELF-LOCALIZATION SYSTEMS

In this system, a smart object equipped with an RFID reader is enabled to localize itself by measuring the backscattered signals obtained from the reference nodes, i.e., chipless tags with known positions as infrastructure [161], [162]. Ranging based on roundtrip time-of-flight (RToF) is carried out using the measured backscattered measurements, and thereafter position can be estimated. RToF based localization is considered at THz frequency region in order to achieve the targeted extremely high localization accuracy, since the available extreme bandwidth offers higher resolution of RToF estimation. Unlike time-based localization in forward-channel systems which requires synchronization between the node and the anchors, RToF based chipless RFID localization offers a great advantage, where RToF ranging utilizes the reader clock and thus does not require clock synchronization between the reader and the tags.

It is shown in [161] the feasibility that RFID based indoor THz self-localization system operated at 100 GHz can achieve sub-mm localization accuracies at several meter read range, where the localization accuracy is improved as the bandwidth of the pulse is increased due to higher resolution of RToF estimation. This system is validated experimentally at microwave frequencies as implemented in [162] under real environments, where the feasibility of the localization system is approved by achieving a higher accuracy within a larger area compared to [158], [176] and references therein.

In [177], effective placement of chipless tags within the indoor environment is proposed to guarantee maximal connectivity between the object and the infrastructure, while considering the system constraints such as: room dimensions, maximum range, tag antenna pattern and its retro-directivity, and link budgets. This algorithm attains the connection at 99% confidence between the object and the required reference chipless tags for self-localization at any location in the indoor environment.

The coverage of RFID backscatter channel at THz band is studied in [161], [177], where the link budget is investigated considering retro-directivity of the chipless tag, THz molecular absorption in addition to the inherent RFID forward and backward path loss. In the aforementioned works, the distance-dependent spectral windows that are feasible for RFID-based localization are characterized. The coverage is validated in [177] for a corner reflector based tag, i.e., shown in Fig. 19, placed at around 18.5 m from the horn antenna opening as shown in Fig. 20. It is clearly noted from Fig. 20, which shows also the measured magnitude of S_{11} compared to the noise level, that the frequency code of the tag represented by the resonance notch can be detected, and a high reflection level from the tag outside the notch is obtained. This level is measured about 12 dB above the noise level. Moreover, the notch has about 25 dB depth, which allows the notch detection at the reader.

C. FUTURE DIRECTIONS

To better exploit the opportunities offered by the THz band for localization systems, many issues and challenges must be considered. More accurate channel modeling is needed that takes into account THz specific problems. Self-interference (SI) from the transmitter to the receiver in the backscattered channel must be considered. In addition, many sources of interference can affect the localization performance, such as reflections from nearby unwanted objects and the

reflected signals from multilayer structures. In addition, the development of THz tags with identification is crucial to achieve better localization coverage. Extending localization algorithms for tracking is crucial for SLAM applications. Moreover, cooperative algorithms between localization and SAR could be used to improve localization accuracy.

VII. CONCLUSION

The field of THz waves has evolved from a basic-science-oriented field to an application-oriented field. In this paper, the advances in the performance and miniaturization of time-domain spectroscopy systems are presented. An important aspect is the choice of laser source. While current commercial THz-TDS systems use low repetition rate fiber lasers, future more compact systems may be based on model-docked high repetition rate semiconductor lasers or superluminescent diodes.

Over the past decade, the sensitivity of THz imaging systems has also improved significantly. In particular, more efficient photoconductive antennas have improved the dynamic range by about 40 dB. In addition, near-field imaging systems have also advanced significantly. A fully integrated 128-pixel system-on-a-chip shows a resolution of 10 μm at 550 GHz. Unlike a THz near-field scanning microscope, the integrated near-field imaging system does not require a precision mechanical positioning element.

Depending on the application, different beam steering/beam shaping concepts have been developed. In the case of phased arrays, optoelectronic beam steering with multiple THz sources has the advantage of providing much greater transmit power. A very simple and inexpensive beamformer is a leaky wave antenna, in which the direction of the transmitted beam is adjusted by changing the carrier frequency.

In terms of fixed wireless access, THz communication systems have demonstrated 100 Gbit/s wireless transmission over a distance of 100 m. Similar cell capacities are being targeted for 6G THz mobile communications, where the leaky wave beamforming concept appears to be very attractive.

In the area of localization, a low-complexity passive and chipless system based on frequency-selective dielectric resonator tags used as anchors for indoor infrastructure is proposed. Using multiple resonators with different resonant frequencies per tag, the tags can be uniquely identified by the interrogation system.

ACKNOWLEDGMENT

The authors would like to thank Open Access Publication Fund of the University of Duisburg-Essen. The authors thank B. Globisch for providing Fig. 6.

REFERENCES

[1] M. Naftaly, N. Vieweg, and A. Deninger, "Industrial applications of terahertz sensing: State of play," *Sensors*, vol. 19, no. 19, 2019, Art. no. 4203, doi: 10.3390/s19194203.

[2] L. Yu et al., "The medical application of terahertz technology in non-invasive detection of cells and tissues: Opportunities and challenges," *RSC Adv.*, vol. 9, no. 17, pp. 9354–9363, 2019, doi: 10.1039/C8RA10605C.

[3] J. C. Bose, "On a self-recovering coherer and the study of the cohering action of different metals author," *Proc. Roy. Soc. Lond.*, vol. 65, pp. 166–172, 1899.

[4] H. Rubens and E. F. Nichols, "Heat rays of great wave length," *Phys. Rev. (Ser. I)*, vol. 4, no. 4, 1897, Art. no. 314.

[5] E. F. Nichols and T. J. D, "Joining the infra-red and electric wave spectra," *Astrophys. J.*, vol. 61, 1925, Art. no. 17.

[6] M. J. Golay, "A pneumatic infra-red detector," *Rev. Sci. Instrum.*, vol. 18, no. 5, pp. 357–362, 1947.

[7] D. Andrews, W. F. Brucksch Jr., W. T. Ziegler, and E. R. Blanchard, "Attenuated superconducting I. For measuring infra-red radiation," *Rev. Sci. Instrum.*, vol. 13, no. 7, pp. 281–292, 1942.

[8] C. A. Burrus and W. Gordy, "Submillimeter wave spectroscopy," *Phys. Rev.*, vol. 93, no. 4, pp. 897–898, Feb. 1954, doi: 10.1103/PhysRev.93.897.

[9] P. Jacquinot, "How the search for a throughput advantage led to Fourier transform spectroscopy," *Infrared Phys.*, vol. 24, no. 2/3, pp. 99–101, May 1984, doi: 10.1016/0020-0891(84)90054-X.

[10] J. W. Cooley and J. W. Tukey, "An algorithm for the machine calculation of complex Fourier series," *Math. Comput.*, vol. 19, no. 90, Apr. 1965, Art. no. 297, doi: 10.2307/2003354.

[11] R. Kompfner and N. Williams, "Backward-wave tubes," *Proc. IRE*, vol. 41, no. 11, pp. 1602–1611, Nov. 1953, doi: 10.1109/JRPROC.1953.274186.

[12] A. Crocker, H. A. Gebbie, M. F. Kimmitt, and L. E. S. Mathias, "Stimulated emission in the far infra-red," *Nature*, vol. 201, no. 4916, pp. 250–251, Jan. 1964, doi: 10.1038/201250a0.

[13] J. E. Chamberlain, J. E. Gibbs, and H. A. Gebbie, "Refractometry in the far infra-red using a two-beam interferometer," *Nature*, vol. 198, no. 4883, pp. 874–875, Jun. 1963, doi: 10.1038/198874b0.

[14] A. M. Nicolson, "Broad-band microwave transmission characteristics from a single measurement of the transient response," *IEEE Trans. Instrum. Meas.*, vol. 17, no. 4, pp. 395–402, Dec. 1968, doi: 10.1109/TIM.1968.4313741.

[15] T. Y. Chang and T. J. Bridges, "Laser action at 452, 496, and 541 μm in optically pumped CH3F," *Opt. Commun.*, vol. 1, no. 9, pp. 423–426, Apr. 1970, doi: 10.1016/0030-4018(70)90169-0.

[16] K. H. Yang, P. L. Richards, and Y. R. Shen, "Generation of far-infrared radiation by picosecond light pulses in $LiNbO_3$," *Appl. Phys. Lett.*, vol. 19, no. 9, pp. 320–323, Nov. 1971, doi: 10.1063/1.1653935.

[17] D. H. Auston, K. P. Cheung, and P. R. Smith, "Picosecond photoconducting Hertzian dipoles," *Appl. Phys. Lett.*, vol. 45, no. 3, pp. 284–286, Aug. 1984, doi: 10.1063/1.95174.

[18] P. H. Siegel, "THz instruments for space," *IEEE Trans. Antennas Propag.*, vol. 55, no. 11, pp. 2957–2965, Nov. 2007, doi: 10.1109/TAP.2007.908557.

[19] C. Kulesa, "Terahertz spectroscopy for astronomy: From comets to cosmology," *IEEE Trans. THz Sci. Technol.*, vol. 1, no. 1, pp. 232–240, Sep. 2011, doi: 10.1109/TTHZ.2011.2159648.

[20] M. van Exter, C. Fattinger, and D. Grischkowsky, "Terahertz time-domain spectroscopy of water vapor," *Opt. Lett.*, vol. 14, no. 20, Oct. 1989, Art. no. 1128, doi: 10.1364/OL.14.001128.

[21] J. B. Bates, "Fourier transform infrared spectroscopy," *Science*, vol. 191, no. 4222, pp. 31–37, Jan. 1976, doi: 10.1126/science.1246596.

[22] P. R. Smith, D. H. Auston, and M. C. Nuss, "Subpicosecond photoconducting dipole antennas," *IEEE J. Quantum Electron.*, vol. 24, no. 2, pp. 255–260, Feb. 1988, doi: 10.1109/3.121.

[23] P. U. Jepsen, D. G. Cooke, and M. Koch, "Terahertz spectroscopy and imaging – Modern techniques and applications," *Laser Photon. Rev.*, vol. 5, no. 1, pp. 124–166, Jan. 2011, doi: 10.1002/lpor.201000011.

[24] M. Bass, P. A. Franken, J. F. Ward, and G. Weinreich, "Optical rectification," *Phys. Rev. Lett.*, vol. 9, no. 11, pp. 446–448, Dec. 1962, doi: 10.1103/PhysRevLett.9.446.

[25] T. Seifert et al., "Efficient metallic spintronic emitters of ultrabroadband terahertz radiation," *Nature Photon.*, vol. 10, no. 7, pp. 483–488, Jul. 2016, doi: 10.1038/nphoton.2016.91.

[26] M. Jazbinsek, U. Puc, A. Abina, and A. Zidansek, "Organic crystals for THz photonics," *Appl. Sci.*, vol. 9, no. 5, Mar. 2019, Art. no. 882, doi: 10.3390/app9050882.

[27] D. J. Cook and R. M. Hochstrasser, "Intense terahertz pulses by four-wave rectification in air," *Opt. Lett.*, vol. 25, no. 16, Aug. 2000, Art. no. 1210, doi: 10.1364/OL.25.001210.

[28] R. L. Fork, B. I. Greene, and C. V. Shank, "Generation of optical pulses shorter than 0.1 psec by colliding pulse mode locking," *Appl. Phys. Lett.*, vol. 38, no. 9, pp. 671–672, May 1981, doi: 10.1063/1.92500.

[29] D. E. Spence, P. N. Kean, and W. Sibbett, "60-fsec pulse generation from a self-mode-locked Ti:Sapphire laser," *Opt. Lett.*, vol. 16, no. 1, Jan. 1991, Art. no. 42, doi: 10.1364/OL.16.000042.

[30] B. B. Hu and M. C. Nuss, "Imaging with terahertz waves," *Opt. Lett.*, vol. 20, no. 16, pp. 1716–1718, 1995, doi: 10.1364/OL.20.001716.

[31] M. E. Fermann, M. Hofer, F. Haberl, A. J. Schmidt, and L. Turi, "Additive-pulse-compression mode locking of a neodymium fiber laser," *Opt. Lett.*, vol. 16, no. 4, pp. 244–246, 1991, doi: 10.1364/OL.16.000244.

[32] B. Sartorius et al., "All-fiber terahertz time-domain spectrometer operating at 1.5 μm telecom wavelengths," *Opt. Exp.*, vol. 16, no. 13, Jun. 2008, Art. no. 9565, doi: 10.1364/OE.16.009565.

[33] R. B. Kohlhaas et al., "Photoconductive terahertz detectors with 105 dB peak dynamic range made of rhodium doped InGaAs," *Appl. Phys. Lett.*, vol. 114, no. 22, Jun. 2019, Art. no. 221103, doi: 10.1063/1.5095714.

[34] D. Damyanov et al., "High resolution lensless terahertz imaging and ranging," *IEEE Access*, vol. 7, pp. 147704–147712, 2019, doi: 10.1109/ACCESS.2019.2934582.

[35] S. Mansourzadeh et al., "High-power lensless THz imaging of hidden objects," *IEEE Access*, vol. 9, pp. 6268–6276, 2021, doi: 10.1109/ACCESS.2020.3048781.

[36] M. Müller et al., "10.4 kW coherently combined ultrafast fiber laser," *Opt. Lett.*, vol. 45, no. 11, Jun. 2020, Art. no. 3083, doi: 10.1364/OL.392843.

[37] P. Russbueldt, T. Mans, J. Weitenberg, H. D. Hoffmann, and R. Poprawe, "Compact diode-pumped 11 kW Yb:YAG Innoslab femtosecond amplifier," *Opt. Lett.*, vol. 35, no. 24, Dec. 2010, Art. no. 4169, doi: 10.1364/OL.35.004169.

[38] J.-P. Negel et al., "Ultrafast thin-disk multipass laser amplifier delivering 14 kW (47 mJ, 1030 nm) average power converted to 820 W at 515 nm and 234 W at 343 nm," *Opt. Exp.*, vol. 23, no. 16, Aug. 2015, Art. no. 21064, doi: 10.1364/OE.23.021064.

[39] F. Meyer, T. Vogel, S. Ahmed, and C. J. Saraceno, "Single-cycle, MHz repetition rate THz source with 66 mW of average power," *Opt. Lett.*, vol. 45, no. 9, May 2020, Art. no. 2494, doi: 10.1364/OL.386305.

[40] J. Buldt, H. Stark, M. Müller, C. Grebing, C. Jauregui, and J. Limpert, "Gas-plasma-based generation of broadband terahertz radiation with 640 mW average power," *Opt. Lett.*, vol. 46, no. 20, Oct. 2021, Art. no. 5256, doi: 10.1364/OL.442374.

[41] E. R. Brown, F. W. Smith, and K. A. McIntosh, "Coherent millimeter-wave generation by heterodyne conversion in low-temperature-grown GaAs photoconductors," *J. Appl. Phys.*, vol. 73, no. 3, pp. 1480–1484, 1993, doi: 10.1063/1.353222.

[42] K. A. McIntosh, E. R. Brown, K. B. Nichols, O. B. McMahon, W. F. DiNatale, and T. M. Lyszczarz, "Terahertz photomixing with diode lasers in low-temperature-grown GaAs," *Appl. Phys. Lett.*, vol. 67, no. 26, pp. 3844–3846, Dec. 1995, doi: 10.1063/1.115292.

[43] L. Liebermeister et al., "Optoelectronic frequency-modulated continuous-wave terahertz spectroscopy with 4 THz bandwidth," *Nature Commun.*, vol. 12, no. 1, Dec. 2021, Art. no. 1071, doi: 10.1038/s41467-021-21260-x.

[44] S. Preu, G. H. Döhler, S. Malzer, L. J. Wang, and A. C. Gossard, "Tunable, continuous-wave terahertz photomixer sources and applications," *J. Appl. Phys.*, vol. 109, no. 6, Mar. 2011, Art. no. 061301, doi: 10.1063/1.3552291.

[45] O. Morikawa, M. Tonouchi, and M. Hangyo, "A cross-correlation spectroscopy in subterahertz region using an incoherent light source," *Appl. Phys. Lett.*, vol. 76, no. 12, 2000, Art. no. 1519, doi: 10.1063/1.126082.

[46] M. Scheller and M. Koch, "Terahertz quasi time domain spectroscopy," *Opt. Exp.*, vol. 17, no. 20, Sep. 2009, Art. no. 17723, doi: 10.1364/OE.17.017723.

[47] K. Merghem, S. F. Busch, F. Lelarge, M. Koch, A. Ramdane, and J. C. Balzer, "Terahertz time-domain spectroscopy system driven by a monolithic semiconductor laser," *J. Infrared, Millimeter, THz Waves*, vol. 38, no. 8, pp. 958–962, Aug. 2017, doi: 10.1007/s10762-017-0401-2.

[48] K. Kolpatzeck et al., "System-theoretical modeling of terahertz time-domain spectroscopy with ultra-high repetition rate mode-locked lasers," *Opt. Exp.*, vol. 28, no. 11, 2020, Art. no. 16935, doi: 10.1364/oe.389632.

[49] T. Göbel, D. Stanze, B. Globisch, R. J. B. Dietz, H. Roehle, and M. Schell, "Telecom technology based continuous wave terahertz photomixing system with 105 decibel signal-to-noise ratio and 35 terahertz bandwidth," *Opt. Lett.*, vol. 38, no. 20, 2013, Art. no. 4197, doi: 10.1364/OL.38.004197.

[50] S. Nellen et al., "Experimental comparison of UTC- and PIN-photodiodes for continuous-wave terahertz generation," *J. Infrared, Millimeter, THz Waves*, vol. 41, pp. 343–354, 2020, doi: 10.1007/s10762-019-00638-5.

[51] R. B. Kohlhaas et al., "Terahertz quasi time-domain spectroscopy based on telecom technology for 1550 nm," *Opt. Exp.*, vol. 25, no. 11, May 2017, Art. no. 12851, doi: 10.1364/OE.25.012851.

[52] D. Molter, M. Kolano, and G. von Freymann, "Terahertz cross-correlation spectroscopy driven by incoherent light from a superluminescent diode," *Opt. Exp.*, vol. 27, no. 9, Apr. 2019, Art. no. 12659, doi: 10.1364/OE.27.012659.

[53] K.-H. Tybussek, K. Kolpatzeck, V. Cherniak, S. Engelbrecht, B. Fischer, and J. C. Balzer, "Spectral shaping of a superluminescent diode for terahertz cross-correlation spectroscopy," *Appl. Sci.*, vol. 12, no. 4, Feb. 2022, Art. no. 1772, doi: 10.3390/app12041772.

[54] D. Decka, G. Schwaab, and M. Havenith, "A THz/FTIR fingerprint of the solvated proton: Evidence for Eigen structure and Zundel dynamics," *Phys. Chem. Chem. Phys.*, vol. 17, no. 17, pp. 11898–11907, 2015, doi: 10.1039/c5cp01035g.

[55] K. Sengupta, T. Nagatsuma, and D. M. Mittleman, "Terahertz integrated electronic and hybrid electronic–photonic systems," *Nature Electron.*, vol. 1, no. 12, pp. 622–635, 2018, doi: 10.1038/s41928-018-0173-2.

[56] J. Hillbrand, A. M. Andrews, H. Detz, G. Strasser, and B. Schwarz, "Coherent injection locking of quantum cascade laser frequency combs," *Nature Photon.*, vol. 13, no. 2, pp. 101–104, 2019, doi: 10.1038/s41566-018-0320-3.

[57] I. E. Gordon et al., "The HITRAN2020 molecular spectroscopic database," *J. Quantitative Spectrosc. Radiative Transfer*, vol. 277, Jan. 2022, Art. no. 107949, doi: 10.1016/j.jqsrt.2021.107949.

[58] C. P. Endres, S. Schlemmer, P. Schilke, J. Stutzki, and H. S. P. Müller, "The cologne database for molecular spectroscopy, CDMS, in the virtual atomic and molecular data centre, VAMDC," *J. Mol. Spectrosc.*, vol. 327, pp. 95–104, Sep. 2016, doi: 10.1016/j.jms.2016.03.005.

[59] T. Kubiczek and J. C. Balzer, "Material classification for terahertz images based on neural networks," *IEEE Access*, vol. 10, pp. 88667–88677, 2022, doi: 10.1109/ACCESS.2022.3200473.

[60] K. Krügener et al., "Terahertz inspection of buildings and architectural art," *Appl. Sci.*, vol. 10, no. 15, pp. 1–17, 2020, doi: 10.3390/app10155166.

[61] A. Bartels et al., "Ultrafast time-domain spectroscopy based on high-speed asynchronous optical sampling," *Rev. Sci. Instrum.*, vol. 78, no. 3, 2007, Art. no. 035107, doi: 10.1063/1.2714048.

[62] K. H. Jin, Y.-G. Kim, S. H. Cho, J. C. Ye, and D.-S. Yee, "High-speed terahertz reflection three-dimensional imaging for nondestructive evaluation," *Opt. Exp.*, vol. 20, no. 23, Nov. 2012, Art. no. 25432, doi: 10.1364/OE.20.025432.

[63] D. Bajek and M. A. Cataluna, "Megahertz scan rates enabled by optical sampling by repetition-rate tuning," *Sci. Rep.*, vol. 11, no. 1, pp. 1–7, 2021, doi: 10.1038/s41598-021-02502-w.

[64] P. Trocha et al., "Ultra-fast optical ranging using quantum-dash mode-locked laser diodes," *Sci. Rep.*, vol. 12, no. 1, pp. 1–10, 2022, doi: 10.1038/s41598-021-04368-4.

[65] J. V. Rudd, D. A. Zimdars, and M. W. Warmuth, "Compact fiber-pigtailed terahertz imaging system," *Proc. SPIE*, vol. 3934, May 2000, Art. no. 27, doi: 10.1117/12.386344.

[66] R. Wilk et al., "THz time-domain spectrometer based on LT-InGaAs photoconductive antennas exited by a 1.55 μm fibre laser," in *Proc. Conf. Lasers Electro-Opt.*, 2007, vol. 1, pp. 1–2, doi: 10.1109/CLEO.2007.4452856.

[67] R. J. B. Dietz et al., "Low temperature grown be-doped InGaAs/InAlAs photoconductive antennas excited at 1030 nm," *J. Infrared, Millimeter, THz Waves*, vol. 34, no. 3/4, pp. 231–237, Apr. 2013, doi: 10.1007/s10762-013-9968-4.

[68] R. B. Kohlhaas et al., "637 μW emitted terahertz power from photoconductive antennas based on rhodium doped InGaAs," *Appl. Phys. Lett.*, vol. 117, no. 13, Sep. 2020, Art. no. 131105, doi: 10.1063/5.0020766.

[69] R. B. Kohlhaas et al., "Ultrabroadband terahertz time-domain spectroscopy using III–V photoconductive membranes on silicon," *Opt. Exp.*, vol. 30, no. 13, Jun. 2022, Art. no. 23896, doi: 10.1364/OE.454447.

[70] A. Soltani, D. Gebauer, L. Duschek, B. M. Fischer, H. Cölfen, and M. Koch, "Crystallization caught in the act with terahertz spectroscopy: Non-classical pathway for L-(+)-tartaric acid," *Chem. A Eur. J.*, vol. 23, no. 57, pp. 14128–14132, Oct. 2017, doi: 10.1002/chem.201702218.

[71] N. Born et al., "Monitoring plant drought stress response using terahertz time-domain spectroscopy," *Plant Physiol.*, vol. 164, no. 4, pp. 1571–1577, Apr. 2014, doi: 10.1104/pp.113.233601.

[72] W. L. Chan, J. Deibel, and D. M. Mittleman, "Imaging with terahertz radiation," *Rep. Prog. Phys.*, vol. 70, no. 8, pp. 1325–1379, 2007, doi: 10.1088/0034-4885/70/8/R02.

[73] D. M. Mittleman, S. Hunsche, L. Boivin, and M. C. Nuss, "T-ray tomography," *Opt. Lett.*, vol. 22, no. 12, Jun. 1997, Art. no. 904, doi: 10.1364/OL.22.000904.

[74] J. P. Guillet et al., "Review of terahertz tomography techniques," *J. Infrared, Millimeter, THz Waves*, vol. 35, no. 4, pp. 382–411, 2014, doi: 10.1007/s10762-014-0057-0.

[75] M. Brucherseifer, P. Haring Bolivar, H. Klingenberg, and H. Kurz, "Angle-dependent THz tomography – Characterization of thin ceramic oxide films for fuel cell applications," *Appl. Phys. B*, vol. 72, no. 3, pp. 361–366, Feb. 2001, doi: 10.1007/s003400100474.

[76] E. Stübling et al., "A THz tomography system for arbitrarily shaped samples," *J. Infrared, Millimeter, THz Waves*, vol. 38, no. 10, pp. 1179–1182, 2017, doi: 10.1007/s10762-017-0415-9.

[77] E.-M. Stübling et al., "Application of a robotic THz imaging system for sub-surface analysis of ancient human remains," *Sci. Rep.*, vol. 9, no. 1, 2019, Art. no. 3390, doi: 10.1038/s41598-019-40211-7.

[78] E.-M. Stubling, N.-A. Staats, B. Globisch, M. Schell, H. D. Portsteffen, and M. Koch, "Investigating the layer structure and insect tunneling on a wooden putto using robotic-based THz tomography," *IEEE Trans. THz Sci. Technol.*, vol. 10, no. 4, pp. 343–347, Jul. 2020, doi: 10.1109/TTHZ.2020.2986652.

[79] R. B. Kohlhaas et al., "Improving the dynamic range of InGaAs-based THz detectors by localized beryllium doping: Up to 70 dB at 3 THz," *Opt. Lett.*, vol. 43, no. 21, Nov. 2018, Art. no. 5423, doi: 10.1364/OL.43.005423.

[80] S. Zhong et al., "Non-destructive quantification of pharmaceutical tablet coatings using terahertz pulsed imaging and optical coherence tomography," *Opt. Lasers Eng.*, vol. 49, no. 3, pp. 361–365, Mar. 2011, doi: 10.1016/j.optlaseng.2010.11.003.

[81] M. Zhai, A. Locquet, C. Roquelet, L. A. Ronqueti, and D. S. Citrin, "Thickness characterization of multi-layer coated steel by terahertz time-of-flight tomography," *NDT E Int.*, vol. 116, Dec. 2020, Art. no. 102358, doi: 10.1016/j.ndteint.2020.102358.

[82] J. L. M. van Mechelen, A. Frank, and D. J. H. C. Maas, "Thickness sensor for drying paints using THz spectroscopy," *Opt. Exp.*, vol. 29, no. 5, pp. 7514–7525, Mar. 2021, doi: 10.1364/OE.418809.

[83] S. Krimi, J. Klier, J. Jonuscheit, G. von Freymann, R. Urbansky, and R. Beigang, "Highly accurate thickness measurement of multi-layered automotive paints using terahertz technology," *Appl. Phys. Lett.*, vol. 109, no. 2, Jul. 2016, Art. no. 021105, doi: 10.1063/1.4955407.

[84] E. Abbe, "Beiträge zur theorie des mikroskops und der mikroskopischen wahrnehmung," *Archiv Für Mikroskopische Anatomie*, vol. 9, no. 1, pp. 418–440, Dec. 1873, doi: 10.1007/BF02956174.

[85] A. J. L. Adam, "Review of near-field terahertz measurement methods and their applications," *J. Infrared, Millimeter, THz Waves*, vol. 32, no. 8/9, pp. 976–1019, Sep. 2011, doi: 10.1007/s10762-011-9809-2.

[86] S. K. Koul and P. Kaurav, "Sub-terahertz and terahertz waves for skin diagnosis and therapy," in *Sub-Terahertz Sensing Technology for Biomedical Applications*. Singapore: Springer Nat. Singapore, 2022, pp. 163–197.

[87] J. Grzyb, B. Heinemann, and U. R. Pfeiffer, "A 0.55 THz near-field sensor with a μm-range lateral resolution fully integrated in 130 nm SiGe BiCMOS," *IEEE J. Solid-State Circuits*, vol. 51, no. 12, pp. 3063–3077, Dec. 2016, doi: 10.1109/JSSC.2016.2603992.

[88] J. Grzyb, B. Heinemann, and U. R. Pfeiffer, "Solid-state terahertz superresolution imaging device in 130-nm SiGe BiCMOS technology," *IEEE Trans. Microw. Theory Techn.*, vol. 65, no. 11, pp. 4357–4372, Nov. 2017, doi: 10.1109/TMTT.2017.2684120.

[89] P. Hillger, J. Grzyb, and U. Pfeiffer, "A fully-integrated terahertz near-field sensor for super-resolution imaging in SiGe BiCMOS," in *Proc. IEEE 41st Int. Conf. Infrared, Millimeter, THz Waves*, 2016, pp. 1–2, doi: 10.1109/IRMMW-THz.2016.7758740.

[90] P. Hillger et al., "A 128-pixel system-on-a-chip for real-time super-resolution terahertz near-field imaging," *IEEE J. Solid-State Circuits*, vol. 53, no. 12, pp. 3599–3612, Dec. 2018, doi: 10.1109/JSSC.2018.2878817.

[91] D. Headland, Y. Monnai, D. Abbott, C. Fumeaux, and W. Withayachumnankul, "Tutorial: Terahertz beamforming, from concepts to realizations," *APL Photon.*, vol. 3, no. 5, 2018, Art. no. 051101, doi: 10.1063/1.5011063.

[92] X. Fu, F. Yang, C. Liu, X. Wu, and T. J. Cui, "Terahertz beam steering technologies: From phased arrays to field-programmable metasurfaces," *Adv. Opt. Mater.*, vol. 8, no. 3, Feb. 2020, Art. no. 1900628, doi: 10.1002/adom.201900628.

[93] B. Ning, Z. Tian, Z. Chen, C. Han, J. Yuan, and S. Li, "Prospective beamforming technologies for ultra-massive MIMO in terahertz communications: A tutorial," 2021, *arXiv:2107.03032*.

[94] H. Jalili and O. Momeni, "A 0.34-THz wideband wide-angle 2-D steering phased array in 0.13-μm SiGe BiCMOS," *IEEE J. Solid-State Circuits*, vol. 54, no. 9, pp. 2449–2461, Sep. 2019, doi: 10.1109/JSSC.2019.2925523.

[95] M. Alonso-delPino, S. Bosma, C. Jung-Kubiak, G. Chattopadhyay, and N. Llombart, "Wideband multimode leaky-wave feed for scanning lens-phased array at submillimeter wavelengths," *IEEE Trans. THz Sci. Technol.*, vol. 11, no. 2, pp. 205–217, Mar. 2021, doi: 10.1109/TTHZ.2020.3038033.

[96] T. P. McKenna, J. A. Nanzer, and T. R. Clark, "Photonic beamsteering of a millimeter-wave array with 10-Gb/s data transmission," *IEEE Photon. Technol. Lett.*, vol. 26, no. 14, pp. 1407–1410, Jul. 2014, doi: 10.1109/LPT.2014.2326332.

[97] K. Kolpatzeck, L. Haring, and A. Czylwik, "Power budget analysis and optimization of photonic beamforming concepts for terahertz transmitters," in *Proc. IEEE German Microw. Conf.*, 2016, pp. 7–10, doi: 10.1109/GEMIC.2016.7461542.

[98] P. Lu et al., "Photonic assisted beam steering for millimeter-wave and THz antennas," in *Proc. IEEE Conf. Antenna Meas. Appl.*, 2018, pp. 1–4, doi: 10.1109/CAMA.2018.8530567.

[99] K. Kolpatzeck, X. Liu, L. Haring, and A. Czylwik, "System-theoretical modeling and analysis of phase control in a photonically steered Terahertz phased array transmitter," in *Proc. 1st Int. Workshop Mobile THz Syst.*, 2018, pp. 1–5, doi: 10.1109/IWMTS.2018.8454691.

[100] D. Headland et al., "Terahertz reflectarrays and nonuniform metasurfaces," *IEEE J. Sel. Topics Quantum Electron.*, vol. 23, no. 4, Jul./Aug. 2017, Art. no. 8500918, doi: 10.1109/JSTQE.2016.2640452.

[101] R. T. Ako, A. Upadhyay, W. Withayachumnankul, M. Bhaskaran, and S. Sriram, "Dielectrics for terahertz metasurfaces: Material selection and fabrication techniques," *Adv. Opt. Mater.*, vol. 8, no. 3, Feb. 2020, Art. no. 1900750, doi: 10.1002/adom.201900750.

[102] A. Diaz-Rubio, S. Kosulnikov, and S. A. Tretyakov, "On the integration of reconfigurable intelligent surfaces in real-world environments: A convenient approach for estimation reflection and transmission," *IEEE Antennas Propag. Mag.*, vol. 64, no. 4, pp. 85–95, Aug. 2022, doi: 10.1109/MAP.2022.3169396.

[103] S. Venkatesh, X. Lu, H. Saeidi, and K. Sengupta, "A programmable terahertz metasurface with circuit-coupled meta-elements in silicon chips: Creating low-cost, large-scale, reconfigurable terahertz metasurfaces," *IEEE Antennas Propag. Mag.*, vol. 64, no. 4, pp. 110–122, Aug. 2022, doi: 10.1109/MAP.2022.3176588.

[104] T. Niu et al., "Experimental demonstration of reflectarray antennas at terahertz frequencies," *Opt. Exp.*, vol. 21, no. 3, Feb. 2013, Art. no. 2875, doi: 10.1364/OE.21.002875.

[105] K. Murano et al., "Low-profile terahertz radar based on broadband leaky-wave beam steering," *IEEE Trans. THz Sci. Technol.*, vol. 7, no. 1, pp. 60–69, Jan. 2017, doi: 10.1109/TTHZ.2016.2624514.

[106] X. Liu et al., "Terahertz beam steering using a MEMS-based reflectarray configured by a genetic algorithm," *IEEE Access*, vol. 10, pp. 84458–84472, 2022.

[107] H. Matsumoto, I. Watanabe, A. Kasamatsu, and Y. Monnai, "Integrated terahertz radar based on leaky-wave coherence tomography," *Nature Electron.*, vol. 3, no. 2, pp. 122–129, Feb. 2020, doi: 10.1038/s41928-019-0357-4.

[108] P. Lu et al., "InP-based THz beam steering leaky-wave antenna," *IEEE Trans. THz Sci. Technol.*, vol. 11, no. 2, pp. 218–230, Mar. 2021, doi: 10.1109/TTHZ.2020.3039460.

[109] Y. Ghasempour, Y. Amarasinghe, C.-Y. Yeh, E. Knightly, and D. M. Mittleman, "Line-of-sight and non-line-of-sight links for dispersive terahertz wireless networks," *APL Photon.*, vol. 6, no. 4, Apr. 2021, Art. no. 041304, doi: 10.1063/5.0039262.

[110] J. Ma, N. J. Karl, S. Bretin, G. Ducournau, and D. M. Mittleman, "Frequency-division multiplexer and demultiplexer for terahertz wireless links," *Nature Commun.*, vol. 8, no. 1, Dec. 2017, Art. no. 729, doi: 10.1038/s41467-017-00877-x.

[111] J. Grajal et al., "3-D high-resolution imaging radar at 300 GHz with enhanced FoV," *IEEE Trans. Microw. Theory Techn.*, vol. 63, no. 3, pp. 1097–1107, Mar. 2015, doi: 10.1109/TMTT.2015.2391105.

[112] K. Sato and Y. Monnai, "Terahertz beam steering based on trajectory deflection in dielectric-free luneburg lens," *IEEE Trans. THz Sci. Technol.*, vol. 10, no. 3, pp. 229–236, May 2020, doi: 10.1109/TTHZ.2020.2983915.

[113] C. Otani, M. Ikari, and Y. Sasaki, "Development of 300 GHz walk-through body scanner for the security gate applications," *Proc. SPIE*, vol. 11827, Aug. 2021, Art. no. 22, doi: 10.1117/12.2594528.

[114] Z. B. Harris, A. Virk, M. E. Khani, and M. H. Arbab, "Terahertz time-domain spectral imaging using telecentric beam steering and an f-θ scanning lens: Distortion compensation and determination of resolution limits," *Opt. Exp.*, vol. 28, no. 18, 2020, Art. no. 26612, doi: 10.1364/oe.398706.

[115] G.-B. Wu, K. F. Chan, S.-W. Qu, and C. H. Chan, "A 2-D beam-scanning Bessel launcher for terahertz applications," *IEEE Trans. Antennas Propag.*, vol. 68, no. 8, pp. 5893–5903, Aug. 2020, doi: 10.1109/TAP.2020.2988936.

[116] R. Piesiewicz et al., "Short-range ultra-broadband terahertz communications: Concepts and perspectives," *IEEE Antennas Propag. Mag.*, vol. 49, no. 6, pp. 24–39, Dec. 2007, doi: 10.1109/MAP.2007.4455844.

[117] T. Kleine-Ostmann and T. Nagatsuma, "A review on terahertz communications research," *J. Infrared, Millimeter, THz Waves*, vol. 32, no. 2, pp. 143–171, 2011, doi: 10.1007/s10762-010-9758-1.

[118] T. Nagatsuma, G. Ducournau, and C. C. Renaud, "Advances in terahertz communications accelerated by photonics," *Nature Photon.*, vol. 10, no. 6, pp. 371–379, 2016, doi: 10.1038/nphoton.2016.65.

[119] I. Kallfass et al., "All active MMIC-based wireless communication at 220 GHz," *IEEE Trans. THz Sci. Technol.*, vol. 1, no. 2, pp. 477–487, Nov. 2011, doi: 10.1109/TTHZ.2011.2160021.

[120] *IEEE Standard for High Data Rate Wireless Multi-Media Networks–Amendment 2: 100 gb/s Wireless Switched Point-To-Point Physical Layer*, IEEE Standard 802.15.3d-2017 (Amendment to IEEE Standard 802.15.3-2016 as amended by IEEE Standard 802.15.3e-2017), Oct. 2017.

[121] V. Petrov, T. Kurner, and I. Hosako, "IEEE 802.15.3d: First standardization efforts for sub-terahertz band communications toward 6G," *IEEE Commun. Mag.*, vol. 58, no. 11, pp. 28–33, Nov. 2020, doi: 10.1109/MCOM.001.2000273.

[122] M. Latva-Aho and K. Leppänen, "Key drivers and research challenges for 6G ubiquitous wireless intelligence," 6G Flagship, Univ. Oulu, Oulu, Finland, Tech. Rep., 2019.

[123] International Telecommunication Union- Radiocommunication Sector, "World Radiocommunication Conference 2019 (WRC-19) final acts," *Electron. Pub. Geneva*, 2020. [Online]. Available: http://www.itu.int/dms_pub/itu-r/oth/12/01/R12010000014A01PDFE.pdf

[124] T. Kurner and A. Hirata, "On the impact of the results of WRC 2019 on THz communications," in *Proc. IEEE 3rd Int. Workshop Mobile THz Syst.*, 2020, pp. 1–3, doi: 10.1109/IWMTS49292.2020.9166206.

[125] S. Koenig et al., "Wireless sub-THz communication system with high data rate," *Nature Photon.*, vol. 7, no. 12, pp. 977–981, 2013, doi: 10.1038/nphoton.2013.275.

[126] T. Merkle et al., "Testbed for phased array communications from 275 to 325 GHz," in *Proc. IEEE Compound Semicond. Integr. Circuit Symp.*, 2017, pp. 1–4, doi: 10.1109/CSICS.2017.8240474.

[127] C. Castro, R. Elschner, T. Merkle, C. Schubert, and R. Freund, "Experimental demonstrations of high-capacity THz-wireless transmission systems for beyond 5G," *IEEE Commun. Mag.*, vol. 58, no. 11, pp. 41–47, Nov. 2020, doi: 10.1109/MCOM.001.2000306.

[128] P. Rodriguez-Vazquez, J. Grzyb, B. Heinemann, and U. R. Pfeiffer, "A QPSK 110-Gb/s polarization-diversity MIMO wireless link with a 220–255 GHz tunable LO in a SiGe HBT technology," *IEEE Trans. Microw. Theory Techn.*, vol. 68, no. 9, pp. 3834–3851, Sep. 2020, doi: 10.1109/TMTT.2020.2986196.

[129] S. Abu-Surra et al., "End-to-end 6G terahertz wireless platform with adaptive transmit and receive beamforming," in *Proc. IEEE Int. Conf. Commun. Workshops*, 2022, pp. 897–903, doi: 10.1109/ICCWorkshops53468.2022.9814579.

[130] (visited 22.11.22). [Online]. Available: https://www.lg.com/my/about-lg/press-and-media/lg-showcases-leadership-in-next-gen-6g-thz-band-demonstration

[131] K. Takano et al., "300-GHz CMOS transmitter module with built-in waveguide transition on a multilayered glass epoxy PCB," in *Proc. IEEE Radio Wireless Symp.*, 2018, pp. 154–156, doi: 10.1109/RWS.2018.8304972.

[132] [Online]. Available: https://thorproject.eu/

[133] D. Wrana, L. John, B. Schoch, S. Wagner, and I. Kallfass, "Sensitivity analysis of a 280–312 GHz superheterodyne terahertz link targeting IEEE802.15.3d applications," *IEEE Trans. THz Sci. Technol.*, vol. 12, no. 4, pp. 325–333, Jul. 2022, doi: 10.1109/TTHZ.2022.3172008.

[134] I. Dan, G. Ducournau, S. Hisatake, P. Szriftgiser, R.-P. Braun, and I. Kallfass, "A terahertz wireless communication link using a superheterodyne approach," *IEEE Trans. THz Sci. Technol.*, vol. 10, no. 1, pp. 32–43, Jan. 2020, doi: 10.1109/TTHZ.2019.2953647.

[135] A. Kunz and X. Zhang, "New 3GPP security features in 5G phase 1," in *Proc. IEEE Conf. Standards Commun. Netw.*, 2018, pp. 1–6, doi: 10.1109/CSCN.2018.8581763.

[136] R. Mohamed, S. Zemouri, and C. Verikoukis, "Performance evaluation and comparison between SA and NSA 5G networks in indoor environment," in *Proc. IEEE Int. Mediterranean Conf. Commun. Netw.*, 2021, pp. 112–116, doi: 10.1109/MeditCom49071.2021.9647621.

[137] M. Alonso-delPino, C. Jung-Kubiak, T. Reck, N. Llombart, and G. Chattopadhyay, "Beam scanning of silicon lens antennas using integrated piezomotors at submillimeter wavelengths," *IEEE Trans. THz Sci. Technol.*, vol. 9, no. 1, pp. 47–54, Jan. 2019, doi: 10.1109/TTHZ.2018.2881930.

[138] X. Liu et al., "Terahertz beam steering concept based on a MEMS-reconfigurable reflection grating," *Sensors*, vol. 20, no. 10, pp. 1–13, 2020, doi: 10.3390/s20102874.

[139] D. Headland, W. Withayachumnankul, R. Yamada, M. Fujita, and T. Nagatsuma, "Terahertz multi-beam antenna using photonic crystal waveguide and Luneburg lens," *APL Photon.*, vol. 3, no. 12, Dec. 2018, Art. no. 126105, doi: 10.1063/1.5060631.

[140] S. Y. Zheng, W. S. Chan, and K. F. Man, "Broadband phase shifter using loaded transmission line," *IEEE Microw. Wireless Compon. Lett.*, vol. 20, no. 9, pp. 498–500, Sep. 2010, doi: 10.1109/LMWC.2010.2050868.

[141] M. Che, Y. Matsuo, H. Kanaya, H. Ito, T. Ishibashi, and K. Kato, "Optoelectronic THz-wave beam steering by arrayed photomixers with integrated antennas," *IEEE Photon. Technol. Lett.*, vol. 32, no. 16, pp. 979–982, Aug. 2020, doi: 10.1109/LPT.2020.3007415.

[142] S. Li, Z. Zhang, B. Rupakula, and G. M. Rebeiz, "An eight-element 140 GHz wafer-scale phased-array transmitter with 32 dBm peak EIRP and >16 Gbps 16QAM and 64QAM operation," in *Proc. IEEE MTT-S Int. Microw. Symp.*, 2021, pp. 795–798, doi: 10.1109/IMS19712.2021.9574953.

[143] M. Urteaga, Z. Griffith, M. Seo, J. Hacker, and M. J. W. Rodwell, "InP HBT technologies for THz integrated circuits," *Proc. IEEE*, vol. 105, no. 6, pp. 1051–1067, Jun. 2017, doi: 10.1109/JPROC.2017.2692178.

[144] A. Stöhr, B. Shih, S. T. Abraha, A. G. Steffan, and A. Ng'oma, "High spectral-efficient 512-QAM-OFDM 60 GHz CRoF system using a coherent photonic mixer (CPX) and an RF envelope detector," in *Proc. Opt. Fiber Commun. Conf.*, Anaheim, CA, USA, Mar. 2016, Paper Tu3B.4, doi: 10.1364/OFC.2016.Tu3B.4.

[145] M. F. Hermelo, P.-T. (Boris) Shih, M. Steeg, A. Ng'oma, and A. Stöhr, "Spectral efficient 64-QAM-OFDM terahertz communication link," *Opt. Exp.*, vol. 25, no. 16, Aug. 2017, Art. no. 19360, doi: 10.1364/OE.25.019360.
[146] M. Steeg, F. Exner, J. Tebart, A. Czylwik, and A. Stohr, "100 Gbit/s V-band transmission enabled by coherent radio-over-fiber system with IF-OFDM envelope detection and SSBI suppression," in *Proc. IEEE 33rd Gen. Assem. Sci. Symp. Int. Union Radio Sci.*, 2020, pp. 1–4, doi: 10.23919/URSIGASS49373.2020.9232159.
[147] J. Tebart, M. Steeg, F. Exner, A. Czylwik, and A. Stöhr, "Frequency-scalable coherent radio-over-fiber architecture for 100 Gbit/s wireless transmission," *URSI Radio Sci. Lett.*, vol. 2, pp. 1–5, 2020, doi: 10.46620/20-0059.
[148] P. Lu et al., "Mobile THz communications using photonic assisted beam steering leaky-wave antennas," *Opt. Exp.*, vol. 29, no. 14, Jul. 2021, Art. no. 21629, doi: 10.1364/OE.427575.
[149] K. Guan et al., "On millimeter wave and THz mobile radio channel for smart rail mobility," *IEEE Trans. Veh. Technol.*, vol. 66, no. 7, pp. 5658–5674, Jul. 2017, doi: 10.1109/TVT.2016.2624504.
[150] V. Petrov et al., "On unified vehicular communications and radar sensing in millimeter-wave and low terahertz bands," *IEEE Wireless Commun.*, vol. 26, no. 3, pp. 146–153, Jun. 2019, doi: 10.1109/MWC.2019.1800328.
[151] H. Sarieddeen, N. Saeed, T. Y. Al-Naffouri, and M.-S. Alouini, "Next generation terahertz communications: A rendezvous of sensing, imaging, and localization," *IEEE Commun. Mag.*, vol. 58, no. 5, pp. 69–75, May 2020, doi: 10.1109/MCOM.001.1900698.
[152] F. Zafari, A. Gkelias, and K. K. Leung, "A survey of indoor localization systems and technologies," *IEEE Commun. Surv. Tut.*, vol. 21, no. 3, pp. 2568–2599, Jul.–Sep. 2019, doi: 10.1109/COMST.2019.2911558.
[153] A. Batra et al., "Short-range SAR imaging from GHz to THz waves," *IEEE J. Microwaves*, vol. 1, no. 2, pp. 574–585, Apr. 2021, doi: 10.1109/JMW.2021.3063343.
[154] X. Yang, Y. Pi, T. Liu, and H. Wang, "Three-dimensional imaging of space debris with space-based terahertz radar," *IEEE Sens. J.*, vol. 18, no. 3, pp. 1063–1072, Feb. 2018, doi: 10.1109/JSEN.2017.2783367.
[155] A. Batra, M. El-Absi, M. Wiemeler, D. Gohringer, and T. Kaiser, "Indoor THz SAR trajectory deviations effects and compensation with passive sub-mm localization system," *IEEE Access*, vol. 8, pp. 177519–177533, 2020, doi: 10.1109/ACCESS.2020.3026884.
[156] S. Gezici et al., "Localization via ultra-wideband radios: A look at positioning aspects for future sensor networks," *IEEE Signal Process. Mag.*, vol. 22, no. 4, pp. 70–84, Jul. 2005, doi: 10.1109/MSP.2005.1458289.
[157] F. Zheng and T. Kaiser, *Digital Signal Processing For RFID*. Hoboken, NJ, USA: Wiley, 2016.
[158] E. Perret, "Displacement sensor based on radar cross-polarization measurements," *IEEE Trans. Microw. Theory Techn.*, vol. 65, no. 3, pp. 955–966, Mar. 2017, doi: 10.1109/TMTT.2016.2638842.
[159] H. Chen, H. Sarieddeen, T. Ballal, H. Wymeersch, M.-S. Alouini, and T. Y. Al-Naffouri, "A tutorial on terahertz-band localization for 6G communication systems," *IEEE Commun. Surv. Tut.*, vol. 24, no. 3, pp. 1780–1815, Jul.–Sep. 2022, doi: 10.1109/COMST.2022.3178209.
[160] H.-J. Song and T. Nagatsuma, "Present and future of terahertz communications," *IEEE Trans. THz Sci. Technol.*, vol. 1, no. 1, pp. 256–263, Sep. 2011, doi: 10.1109/TTHZ.2011.2159552.
[161] M. El-Absi, A. A. Abbas, A. Abuelhaija, F. Zheng, K. Solbach, and T. Kaiser, "High-accuracy indoor localization based on chipless RFID systems at THz band," *IEEE Access*, vol. 6, pp. 54355–54368, 2018, doi: 10.1109/ACCESS.2018.2871960.
[162] M. El-Absi, A. A. Abbas, A. Abuelhaija, K. Solbach, and T. Kaiser, "Chipless RFID infrastructure based self-localization: Testbed evaluation," *IEEE Trans. Veh. Technol.*, vol. 69, no. 7, pp. 7751–7761, Jul. 2020, doi: 10.1109/TVT.2020.2990480.
[163] A. Jiménez-Sáez et al., "Frequency-coded mm-wave tags for self-localization system using dielectric resonators," *J. Infrared, Millimeter, THz Waves*, vol. 41, no. 8, pp. 908–925, 2020, doi: 10.1007/s10762-020-00707-0.
[164] A. Alhaj Abbas, M. El-Absi, A. Abuelhaija, K. Solbach, and T. Kaiser, "RCS enhancement of dielectric resonator tag using spherical lens," *Frequenz*, vol. 73, no. 5/6, pp. 161–170, 2019, doi: 10.1515/freq-2018-0224.
[165] A. Alhaj Abbas, M. El-Absi, A. Abualhijaa, K. Solbach, and T. Kaiser, "Dielectric resonator-based passive chipless tag with angle-of-arrival sensing," *IEEE Trans. Microw. Theory Techn.*, vol. 67, no. 5, pp. 2010–2017, May 2019, doi: 10.1109/TMTT.2019.2901447.
[166] A. Alhaj Abbas, M. El-Absi, A. Abuelhaija, K. Solbach, and T. Kaiser, "Corner reflector tag with RCS frequency coding by dielectric resonators," *IET Microw., Antennas Propag*, vol. 15, no. 6, pp. 560–570, 2021, doi: 10.1049/mia2.12067.
[167] A. A. Abbas, M. H. Hassan, A. Abuelhaija, D. Erni, K. Solbach, and T. Kaiser, "Retrodirective dielectric resonator tag with polarization twist signature for clutter suppression in self-localization system," *IEEE Trans. Microw. Theory Techn.*, vol. 69, no. 12, pp. 5291–5299, Dec. 2021, doi: 10.1109/TMTT.2021.3108151.
[168] A. Alhaj Abbas, M. El-Absi, A. Abuelhaija, K. Solbach, and T. Kaiser, "High RCS passive tag based on dielectric resonator - 2D lens combination," in *Proc. 12th German Microw. Conf.*, 2019, pp. 5–8, doi: 10.23919/GEMIC.2019.8698178.
[169] C. R. Tubío, J. A. Nóvoa, J. Martín, F. Guitián, J. R. Salgueiro, and A. Gil, "3D printing of Al_2O_3 photonic crystals for terahertz frequencies," *RSC Adv.*, vol. 6, no. 3, pp. 2450–2454, 2016, doi: 10.1039/C5RA22737B.
[170] P. Kadera, A. Jimenez-Saez, T. Burmeister, J. Lacik, M. SchusBler, and R. Jakoby, "Gradient-index-based frequency-coded retroreflective lenses for mm-wave indoor localization," *IEEE Access*, vol. 8, pp. 212765–212775, 2020, doi: 10.1109/ACCESS.2020.3039986.
[171] M. Bernier, F. Garet, E. Perret, L. Duvillaret, and S. Tedjini, "Terahertz encoding approach for secured chipless radio frequency identification," *Appl. Opt.*, vol. 50, no. 23, Aug. 2011, Art. no. 4648, doi: 10.1364/AO.50.004648.
[172] Y. Kujime, M. Fujita, and T. Nagatsuma, "Terahertz tag using photonic-crystal slabs," *J. Lightw. Technol.*, vol. 36, no. 19, pp. 4386–4392, Oct. 2018, doi: 10.1109/JLT.2018.2825464.
[173] M. I. W. Khan et al., "CMOS THz-ID: A 1.6-mm^2 package-less identification tag using asymmetric cryptography and 260-GHz far-field backscatter communication," *IEEE J. Solid-State Circuits*, vol. 56, no. 2, pp. 340–354, Feb. 2021, doi: 10.1109/JSSC.2020.3015717.
[174] Y. Amarasinghe, H. Guerboukha, Y. Shiri, and D. M. Mittleman, "Bar code reader for the THz region," *Opt. Exp.*, vol. 29, no. 13, Jun. 2021, Art. no. 20240, doi: 10.1364/OE.428547.
[175] Y. Guan, M. Yamamoto, T. Kitazawa, S. R. Tripathi, K. Takeya, and K. Kawase, "A concealed barcode identification system using terahertz time-domain spectroscopy," *J. Infrared, Millimeter, THz Waves*, vol. 36, no. 3, pp. 298–311, Mar. 2015, doi: 10.1007/s10762-014-0128-2.
[176] R.-E.-A. Anee and N. C. Karmakar, "Chipless RFID tag localization," *IEEE Trans. Microw. Theory Techn.*, vol. 61, no. 11, pp. 4008–4017, Nov. 2013, doi: 10.1109/TMTT.2013.2282280.
[177] M. El-Absi, A. Al-Haj Abbas, and T. Kaiser, "Chipless RFID tags placement optimization as infrastructure for maximal localization coverage," *IEEE J. Radio Freq. Identification*, vol. 6, pp. 368–380, 2022, doi: 10.1109/JRFID.2022.3189555.

JAN C. BALZER (Member, IEEE) received the Dipl.-Ing. (FH) degree in telecommunications from Dortmund University of Applied Sciences, Dortmund, Germany, in 2008, and the Master of Science degree in electrical engineering and information technology and the Dr.-Ing. degree from Ruhr University Bochum, Bochum, Germany, in 2010 and 2014, respectively. In 2015, he has joined the Research Group of Prof. Martin Koch, Philipp University of Marburg, Marburg, Germany, as a Postdoctoral Fellow. Since 2017, he has been an Assistant Professor of terahertz systems with the Faculty of Engineering, University of Duisburg-Essen, Duisburg, Germany. His scientific research focuses on ultrafast semiconductor lasers. From here, he moved to the field of terahertz radiation generation and applications. He made contributions in the field of compact laser diode-driven THz systems, 3D-printed THz devices, high-resolution THz imaging, and THz material characterization.

CLARA J. SARACENO received the Diploma in engineering and the M.Sc. degree from Institut d'Optique Graduate School, Paris, France, in 2007, and the Ph.D. degree in physics from ETH Zürich, Zürich, Switzerland, in 2012, with in the Group of Prof. Ursula Keller, where she carried out research on ultrafast disk lasers and their use for high harmonics generation. From 2013 to 2014, she was a Postdoctoral Fellow with the University of Neuchatel, Neuchâtel, Switzerland, and ETH Zürich, followed by a Postdoc position from 2015 to 2016 with ETH Zürich. She was an Associate Professor of photonics and ultrafast science with the Electrical Engineering Faculty, Ruhr University Bochum, Bochum, Germany. Since 2020, she has been a Full Professor with Ruhr University Bochum. Research topics of her group include high-power ultrafast lasers and terahertz science and technology. She was elected Fellow of Optica (formerly the Optical Society). She was the recipient of the ETH Medal for her Ph.D. dissertation, European Physical Society (Quantum Electronics and Optics Division) Thesis Prize in applied aspects in 2013, Sofja Kovalevskaja Award of the Alexander von Humboldt Foundation in 2016, and an ERC Starting Grant and in 2021.

MARTIN KOCH received the Diploma and Ph.D. degree in physics from Philipps-Universität Marburg, Marburg, Germany, in 1991 and 1995, respectively. From 1995 to 1996, he was a Postdoctoral Fellow with Bell Labs/Lucent Technologies, Holmdel, NJ, USA. From 1996 to 1998, he was with the Photonics and Optoelectronics Group, University of Munich, Munich, Germany. Since 1998, he has been an Associate Professor with the Department of Electrical Engineering, Technische Universität Braunschweig, Braunschweig, Germany. In 2003, he spent a three-month sabbatical with the University of California Santa Barbara, Santa Barbara, CA, USA. Since 2009, he has been a Professor of experimental semiconductor physics with the Philipps-Universität Marburg. Prof. Koch was the recipient of the Kaiser-Friedrich Research Prize in 2003, IPB Patent Award in 2009, and Exceptional Service Award of the IRMMW-THz Society in 2019. He is currently the Editor-in-Chief of *Journal of Infrared, Millimeter, and Terahertz Waves*.

PRIYANSHA KAURAV received the B.Tech. degree in electronics from the Indian Institute of Information Technology, Design and Manufacturing, Jabalpur, India, in 2015, the M.Tech. degree in RF and microwave engineering from the Indian Institute of Technology (IIT) Delhi, New Delhi, India, in 2017, and the Ph.D. degree from the Centre for Applied Research in Electronics, IIT Delhi, in 2022. From 2017 to 2018, she was an RFiC Design Engineer with Qualcomm, San Diego, CA, USA. She is currently a Postdoctoral Researcher and a Group Leader in terahertz remote sensing and imaging with the Institute for High-Frequency and Communication Technology, Wuppertal, Germany. Her research interests include investigating possible applications of millimeter and terahertz wave imaging systems in the biomedical domain. She was the recipient of the prestigious Prime Minister's Research Fellowship for pursuing her research in the field of terahertz.

ULLRICH R. PFEIFFER (Fellow, IEEE) received the Diploma and Ph.D. degree in physics from the University of Heidelberg, Heidelberg, Germany, in 1996 and 1999, respectively. In 1997, he was a Research Fellow with the Rutherford Appleton Laboratory, Oxfordshire, England. From 1999 to 2001, he was a Postdoctoral Researcher with the University of Heidelberg on real-time electronics for particle physics experiments with the European Organization for Nuclear Research, Geneva, Switzerland. From 2001 to 2006, he was with the IBM T.J. Watson Research Center, Ossining, NY, USA, where his research involved RF circuit design, power amplifier design at 60GHz and 77GHz, high-frequency modeling and packaging for millimeter-wave communication systems. In 2007, he led the THz Electronics Group, Institute of High-Frequency and Quantum Electronics, University of Siegen, Siegen, Germany. Since 2008, he has been the High-Frequency and Communication Technology Chair with the University of Wuppertal, Wuppertal, Germany. From 2016 to 2017, he was the President of the German Association (Fakultätentag) of electrical engineering and information technology e.V. (FTEI), Germany. He has authored and coauthored more than 200 publications and is a Principal Inventor and co-inventor of more than 10 U.S. and international issued patents, relating to RF, millimeter-wave, terahertz communication/imaging circuits and sensors. During 2014–2015, he was an IEEE SSCS Distinguished Lecturer. He served on several IEEE technical program committees, such as the International Solid-State Circuits Conference. Among other awards, he was the recipient of the 2007 European Young Investigator Award, a 2021 ERC Advanced Grant, and EuMC Microwave Prize and MTT Microwave in 2017. He was a co-recipient of the 2004 and 2006 Lewis Winner Award, and 2012 and 2018 Jan Van Vessem Award at the ISSCC Conference.

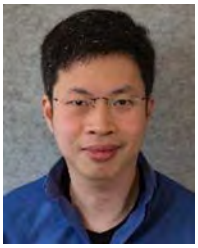

WITHAWAT WITHAYACHUMNANKUL (Senior Member, IEEE) received the bachelor's and master's degrees in electronic engineering from the King Mongkut's Institute of Technology Ladkrabang, Bangkok, Thailand, in 2001 and 2003, respectively, and a Doctorate degree in electrical engineering with a Dean's Commendation from The University of Adelaide, Adelaide, SA, Australia, in 2010. He is currently an Associate Professor with the University of Adelaide, and a Leader of the Terahertz Engineering Laboratory. Since 2017, he has been a Visiting Researcher with Osaka University, Suita, Japan. He has authored and coauthored more than 100 journal publications. In recent years, he has been the Lead Investigator of four Australian Research Council grants, totalling to over AUD 1.5 million. His research interests include terahertz waveguides, metasurfaces, antennas, radar, communications, metrology, and non-destructive evaluation. In 2015, he was a Research Fellow of the Japan Society for the Promotion of Science with the Tokyo Institute of Technology, Tokyo, Japan. He is currently the Track Editor of IEEE TRANSACTIONS ON TERAHERTZ SCIENCE AND TECHNOLOGY. Between 2017 and 2018, he was the Chair of the IEEE South Australia Joint Chapter on Microwave Theory and Techniques and Antennas and Propagation. He was the recipient of a 3-year Australian Research Council Postdoctoral Fellowship in 2010 and IRMMW-THz Society Young Scientist Award 2020.

THOMAS KÜRNER (Fellow, IEEE) received the Dipl.-Ing. degree in electrical engineering and the Dr.-Ing. degree from the University of Karlsruhe, Karlsruhe, Germany. From 1990 to 1994, he was with the Institut für Höchstfrequenztechnik und Elektronik, University of Karlsruhe, working on wave propagation modeling, radio channel characterization, and radio network planning. From 1994 to 2003, he was with the Radio Network Planning Department, headquarters of the GSM 1800 and UMTS operator E-Plus Mobilfunk GmbH & Co KG, Düsseldorf, Germany, where he was a Team Manager radio network planning support responsible for radio network planning tools, algorithms, processes and parameters from 1999 to 2003. Since 2003, he has been a Full University Professor of mobile radio systems with the Technische Universität Braunschweig, Braunschweig, Germany. In 2012, he was a Guest Lecturer with Dublin City University, Dublin, Ireland, within the Telecommunications Graduate Initiative in Ireland. He is currently chairing the IEEE 802.15 Standing Committee THz. He was also the Chair of IEEE 802.15.3d TG 100G, which developed the worldwide first wireless communications standard operating at 300 GHz. He was also a Project Coordinator of the H2020-EU-Japan Project ThoR (TeraHertz end-to-end wireless systems supporting ultra-high data rate applications) and Coordinator of the German DFG-Research Unit FOR 2863 Meteracom (Metrology for THz Communications). He was the recipient of the Neal-Shephard Award of the IEEE Vehicular Technology Society between 2019 and 2022. From 2016 to 2021, he was a member of the Board of Directors of the European Association on Antennas and Propagation and from 2020 to 2022, a Distinguished Lecturer of the IEEE Vehicular Technology Society.

ANDREAS STÖHR (Senior Member, IEEE) received the Dipl.-Ing. and Dr.-Ing. degrees in electrical engineering from Gerhard-Mercator-University, Duisburg, Germany, in 1991 and 1997, respectively. From 1987 to 1996, he was the CEO of MS Steuerungsanlagen GmbH, Kerpen, Germany. From 1996 to 2011, he was with University Duisburg-Essen, Duisburg. Since 2011, he has been the Head of the Center for Semiconductor Technology and Optoelectronics (ZHO), Optoelectronics Department, University Duisburg-Essen. Since 2019, he has been the Co-founder and CEO of Microwave Photonics GmbH, Oberhausen, Germany. Between 1998 and 1999, he joined the National Institute for Information and Communications Technology, Tokyo, Japan, where he worked on 60 GHz wireless systems employing radio over fiber techniques. Since 2015, he has been with Corning Inc., Corning, NY, USA, working on mm-wave and THz communications. From 2015 to 2016, he was a Visiting Professor with the University of Ottawa, Ottawa, ON, Canada. He has authored or coauthored more than 200 papers in refereed journals and conferences. His research interests include the photonic integrated circuits for microwave photonic applications and THz photonics for imaging, spectroscopy and communications. He is currently a Senior Member in IEEE Photonics and MTT societies and Member of the German VDE ITG Fachausschuss KT3 Optische Nachrichtentechnik. He has served on several program committees for international conferences. Prof. Stöhr is a Steering Committee Member of the German DFG Collaborative Research Program MARIE targeting mobile THz material science and represents University Duisburg-Essen in two German 6G hubs 6GEM and Open6GHub.

MOHAMMED EL-ABSI received the B.E. degree in electrical engineering from the Islamic University of Gaza, Gaza, Palestine, in 2005, the M.S. degree in electrical engineering from Jordan University of Science and Technology, Irbid, Jordan, in 2008, and the Ph.D. degree (*summa cum laude*) in electrical engineering from the University of Duisburg-Essen, Duisburg, Germany, in 2015. He is currently a Senior Researcher with Digital Signal Processing Institute, University of Duisburg-Essen. He is also a Principal Investigator with terahertz.NRW research network. He is currently contributing in 6G research hub for open, efficient and secure mobile radio systems (6GEM) and Collaborative Research Center Mobile Material Characterization and Localization by Electromagnetic Sensing (MARIE). His research interests include communication and signal processing. He was the recipient of Mercator Fellow at the Collaborative Research Center Mobile Material Characterization and Localization by Electromagnetic Sensing (MARIE) during 2017–2018 and German Academic Exchange Service Fellowship between 2006 and 2011.

ALI AL-HAJ ABBAS received the B.Sc. degree in electrical/communication engineering from Yarmouk University, Irbid, Jordan, in 2010, the M.Sc. degree in electrical/communication engineering from the University of Jordan, Amman, Jordan, in 2016, and the Ph.D. degree from the University of Duisburg-Essen, Duisburg, Germany, in 2020. From March 2011 to July 2017, he was a Teaching Assistant and Lecturer with Applied Science Private University, Amman. He is currently a Researcher with the Collaborative Research Center for the project Mobile Material Characterization and Localization by Electromagnetic Sensing (MARIE), Institute of Digital Signal Processing (DSV), University of Duisburg-Essen. His research interests include antennas, photonic crystal, terahertz identification, ulrawideband antennas, and chipless radio frequency identification tags.

THOMAS KAISER (Senior Member, IEEE) received the Diploma in electrical engineering from Ruhr-University Bochum, Bochum, Germany, in 1991, and the Ph.D. (with distinction) and German Habilitation degrees in electrical engineering from Gerhard Mercator University, Duisburg, Germany in 1995 and 2000, respectively. From 1995 to 1996, he spent a research leave with the University of Southern California, Los Angeles, CA, USA, which was grant-aided by the German Academic Exchange Service. From April 2000 to March 2001, he was the Head of the Department of Communication Systems, Gerhard Mercator University, and from April 2001 to March 2002, he was the Head of the Department of Wireless Chips and Systems, Fraunhofer Institute of Microelectronic Circuits and Systems, Duisburg. From April 2002 to July 2006, he was a co-leader of the Smart Antenna Research Team, University of Duisburg-Essen, Duisburg. In summer 2005, he joined the Smart Antenna Research Group, Stanford University, Stanford, CA, USA, as a Visiting Professor, and in winter 2007, he joined the Department of Electrical Engineering, Princeton University, Princeton, NJ, USA, as a Visiting Professor. From 2006 to 2011, he headed the Institute of Communication Technology, Leibniz University of Hannover, Hanover, Germany. He heads the Institute of Digital Signal Processing, University of Duisburg-Essen and is the founder and CEO of ID4us GmbH, an RFID centric company. He is the author and coauthor of more than 350 papers in international journals and conference proceedings and two books titled *Ultra Wideband Systems With MIMO* (Wiley, 2010) and *Digital Signal Processing for RFID* (Wiley, 2015), and he is the Speaker of the Collaborative Research Center *Mobile Material Characterization and Localization by Electromagnetic Sensing* (MARIE). Dr. Kaiser was the Founding Editor-in-Chief of the e-letter of the IEEE Signal Processing Society and General Chair of the IEEE International Conference on UltraWideBand in 2008, International Conference on Cognitive Radio Oriented Wireless Networks and Communications in 2009, IEEE Workshop on Cellular Cognitive Systems in 2014, and IEEE Workshop on Mobile THz Systems during 2018–2022. He also co-founded several hightech-startups.

ANDREAS CZYLWIK received the Dr.-Ing. and Habilitation degrees in optical communications from the Technical University of Darmstadt, Darmstadt, Germany, in 1988 and 1994, respectively. From 1978 to 1983, he studied electrical engineering with the Technical University of Darmstadt. From 1994 to 2000, he was with the Research and Development Center (Technologiezentrum), Department of Local Area Broadband Radio Systems, Deutsche Telekom, Bonn, Germany. In 2000, he became a Full Professor with the Technical University of Braunschweig, Braunschweig, Germany, heading the Research Group of Microcellular Radio Systems. Since 2002, he has been with the University of Duisburg-Essen, Duisburg, Germany, heading the Chair of Communication Systems. His research interests include radio communications on link and system level with special focus on adaptive multicarrier MIMO techniques. His several research activities focuses on utilizing high frequency (up to THz) electromagnetic waves with applications in the field of extreme wideband communications and radar systems. His current research intereste include the application of radio communications in the field of technical security systems. Since 2014, Dr. Czylwik has been the Chairperson of EUSAS and the European Society for Automatic Alarm Systems.